

Review of “Observations and Comparisons of Cloud Microphysical Properties in Spring and Summertime Arctic Stratocumulus during the ACCACIA campaign.” By Lloyd et al.

This paper details observations from a recent field experiment where aircraft sampled mixed phase clouds and aerosol properties in the vicinity of Svalbard. Overall, I think the results could be an important contribution to research in arctic mixed phase cloud microphysics, but some extensive revisions to the paper are needed before I would determine it to be fit for publication in ACP. In particular, I think the introduction does not pay enough attention to some studies regarding aerosol indirect effects with regards to mixed phase clouds, and I think explaining their results in the context of these studies would be of great benefit to the paper. Furthermore, the paper goes into gory detail about 4 different flights, listing off many data points that do not have a whole lot of relevance to the paper’s main arguments as a whole, particularly in Sections 3 to 7 where many of the details can be cut out and either integrated into the discussion section. If an integration is not desired, then these points could be more eloquently expressed as a figure as I will show in the comments. The paper is also quite wordy, and I highly urge the authors to make the paper more concise. There is also a fundamental problem with quoting 1 Hz values of ice concentrations in that the sample statistics may be inadequate given the relatively low number of ice particles sampled over 60-100 m by the probes, so the given 0.1 Hz observations are more appropriate for use. Furthermore, the conclusion section lacks any details about what is recommended for future studies, which should be noted. Detailed comments about each section are listed below.

Section 1: A much greater amount of detail is necessary in your description of how CCN and IN can affect cloud properties. In particular, there are three different hypotheses listed by Lohmann and Feichter (2005) and in Figure 1 of Jackson et al. (2012) for how CCN and IN affect mixed phase cloud properties:

1. The thermodynamic indirect effect hypothesizes that increasing CCN leads to a decrease in droplet sizes. This decrease in droplet sizes decreases the number of drizzle drops necessary for rime-splintering to occur and hence leads to a reduction in the number of ice crystals due to suppression of secondary ice production. (Rangno and Hobbs 2001)
2. The glaciation indirect effect states that an increase in IN leads to an increase in the number of ice crystals (Lohmann et al. 2001).
3. The riming indirect effect states that increasing CCN decreases the droplet size and hence inhibits growth of ice crystals via riming, decreasing the IWC. (Borys et al. 2003)

These three hypothesis have been stated in the introduction (*lines 60-69*) and discussed in relation to our work in the discussion (*line 483-488;600-603;615-617*). We didn't find evidence that increased CCN was leading to a suppression of secondary ice production. However comparing spring case 1 and 2 (low and high aerosol loadings respectively) there is support for the riming indirect effect. In case 1 IWC values were higher than in the second spring case (approximately a factor of 2 or 3).

Although we didn't make direct IN measurements we infer that ice number concentrations in both Antarctic and Arctic clouds outside the HM temperature zone were controlled by

primary heterogeneous ice nucleation. Concentrations were lower in the Antarctic when compared to the Arctic and this is likely to be a manifestation of the glaciation indirect effect where increased IN availability in the Arctic has led to higher concentrations of ice here when compared to the Antarctic.

You should mention the Lance et al. (2011) and Jackson et al. (2012) papers looking at ARCTAS and ISDAC as well. The comparisons made in the paper should also be discussed in terms of these three hypotheses and what the relative impact of each effect is for the case you are presenting.

These papers have now been cited and discussed in the paper (*lines 70-91*)

Lines 25-29, page 28760: These lines are not referenced, although probably are not needed either since you have already demonstrated that single and multi-layer mixed phase clouds exist and have a wide variation in properties.

The lines refer to work discussed in the Verlinde et al. (2007) paper, however I've removed these lines as suggested.

Objective 2: Why compare your ice concentrations against the DeMott parameterization? I don't think this was adequately explained in the introduction.

The aim is to compare predicted ice nuclei concentrations in these clouds with in-situ measurements from the microphysics probes used in this study. Primary ice nucleation parameterisations are an important aspect of cloud modelling and we think it's useful to compare these with in-situ observations of cloud ice concentrations. A paragraph has been added in the introduction to describe this. (*lines 94-99*)

Lines 7, page 28762: Why weren't the other cases selected? Surely they have some variability in aerosol loadings that can be examined. Since the overall goal is to select two cases that have a comparable meteorological setup and surface conditions with different aerosol loadings, the selection of these two cases needs to be better justified in terms of the meteorological and surface conditions as well as the aerosol loadings. It may do some good to present the synoptic conditions that formed these clouds as well as to mention whether the clouds were over land, ice, or open water since these factors can play a role in determining the microphysical properties.

The two spring cases represented this variability in aerosol loadings and were selected to see if this impacted on the cloud microphysics. The rationale for selecting each case is described in the manuscript (*pages 150-159*). One case had much higher concentrations compared to the other, and the most notable impact this had on cloud properties involved the liquid phase, with no significant changes in the ice phase between the two cases. Presumably the aerosol in the increased loadings case were not IN active, or at least not IN active in the temperature range these clouds spanned.

The summer cases were selected specifically to address the impact of secondary ice production on the cloud layers. Other cases were found to be less conducive for secondary ice production through rime-splintering due to the temperature of the cloud layers.

Spring case one and two took place mainly over ocean and mainly over the ice or marginal ice zone respectively. The summer cases were conducted over the ocean. Although the aims of the flight were to fly over ice and over water the eventual outcome was actually that the surface below was generally similar for each case (either over water or over ice). For this reason the paper does not aim to address the differences in microphysical structure depending on whether the clouds are over the ice or over the ocean. In the case introductions I've removed the actual aims of the flight and described only what was carried out as this can be confusing.

Referee 2 also requested more detail about the synoptic conditions, we have added more detail about this at the beginning of each case study.

Line 16-20, page 28763: I would suggest removing these two sentences since these probes are not used in the paper.

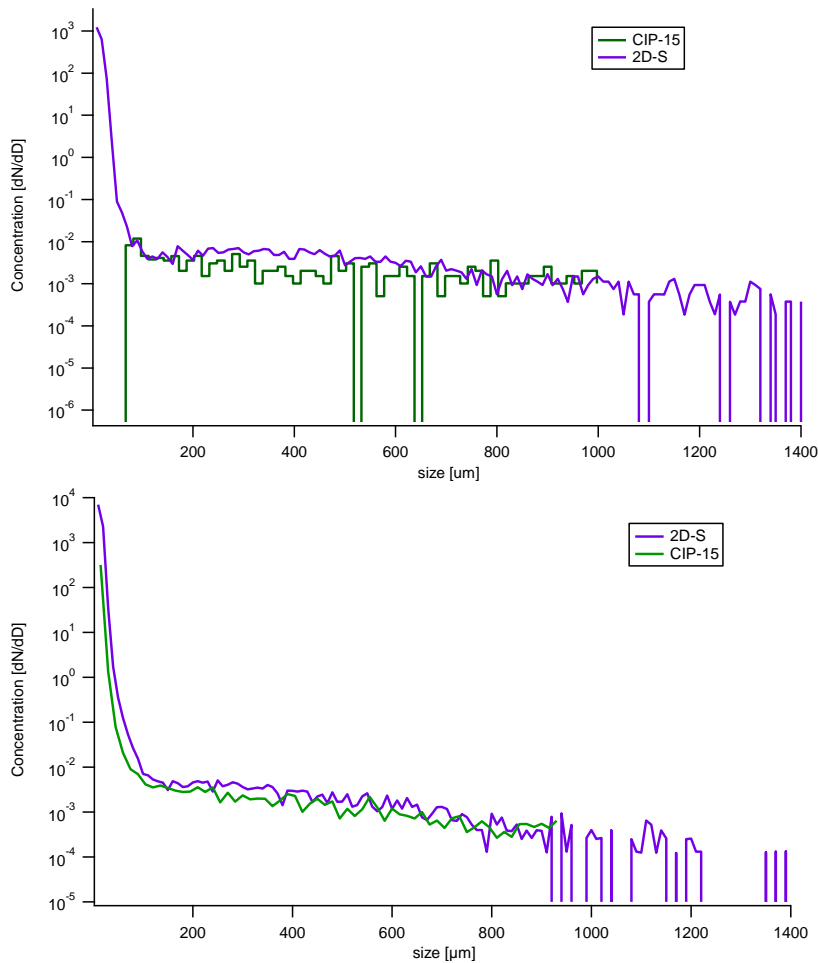
These lines have been removed.

Line 9-11, page 28764: Remove, since you mention this later.

This has been removed.

Line 12-17, page 28764: I don't think you mention the size ranges where you use the CIP-100 in place of the 2DS data. For what size ranges do you use the CIP-100 and 2DS? The resolution of the CIP-15 and the 2DS probes is comparable, and the response time should only affect the sampling of the smallest particles, so a comparison of the CIP-15 and 2D-S concentrations in their overlapping size ranges is needed in order to justify the choices of probes for each size range and to provide the reader an idea of how different the measurements from the differing probes are.

We had the ability to compare the 2D-S and CIP-15 instruments during the spring only, and found good agreement in their size distributions. We haven't included a new figure in the paper showing this but have added text to state this. (*lines 203-204*) We also include an example figure in this response (below) showing the comparison of the two instruments for a period during Spring Case 1 and Spring Case 2 respectively.



In the spring cases we used the 2D-S to 1050 microns and then extended this range using the CIP-100 (upto 6200 microns) to capture the larger particles that could contribute significantly to the ice water content.

Line 19-20, page 28764: You need to justify why you are using the Brown and Francis (1996) relationship here. Since the appropriate relationship depends on particle habit, you need to justify your choice based on the particle habits that were observed. Many studies use an automated habit identification scheme to determine what percentage of particles in a given size range are of a particular habit and then calculate the total mass of particles in a habit category. The final IWC is then the sum of the mass of particles over all categories. Another method that takes particle habit into account is in Baker and Lawson (2006). In any case, further justification of your choice of m-D relationship is required.

Brown and Francis is still widely used in the literature to estimate ice water mass in mixed phase clouds eg Crosier et al (2011). Other studies such as Baker and Lawson referred to be the referee have found discrepancies between their treatments of the data and Brown and Francis when crystals are large and have low aspect ratio with relatively good agreement for smaller crystals with larger aspect ratio. In most of the clouds studied where the ice water mass is large it is dominated by crystals smaller than 100 μm by particles with a high aspect ratio in which good agreement is found between Brown and Francis compared to Baker and Lawson. In view of the crystal habits and size observed in this work and for consistency with previous studies we have used Brown and Francis.

Line 121, 28764: Probably should cite Korolev et al. (2013).

This citation has been added to the text.

Line 9, 28765: Could you define “majority” 50%, 80%?

The IAT thresholds were chosen by looking at the IAT histograms for different regions of microphysics. The majority means that the selected IAT threshold value would likely remove the vast majority of shattered particles as the shattering mode was well separated from the mode of good particles centred at higher IAT time values.

Lines 10-215, 28765: You do not need to mention this here.

This section has been removed.

Line 17-18, 28765: Was there a Continuous Flow Diffusion Chamber or similar instrument to directly measure IN? I think you need to mention that the parameterization is used in place of direct measurements of IN direct measurements if they are not available.

Direct IN measurements were not made, and information about this has been included and explain the use of DeMott et al. (2010). (*lines 94-99 and line 254*)

Line 220-24, 28765: What relative humidity thresholds were used? Plus, shattering of ice crystals on the sample tubes/inlets could potentially contaminate PCASP+CAS measurements at the large end of the size range. Did you take care to not include concentrations in time periods where there were ice crystals present in the 2DS/CIP data to help reduce this contamination? Furthermore, how were the PCASP and CAS measurements combined together?

The aerosol was measured during out of cloud periods containing no hydrometeors together with suitably low RH values. The maximum RH values for each measurement period are given in Table 3. The PCASP and CAS measurements were used independently for input into the ice nucleation scheme.

Sections 3 to 6 and appendices: These sections give an extensive list of small details of several flights that do not add much to the overarching conclusions of the paper. I recommend that either this section be condensed to only mention the overall structure of the cases encountered, or that the details needed from this section to support your conclusions be mentioned in the discussion. It may even help to simply create figures that give an approximate picture of the cloud, like for example, Figure 9 of Jackson et al. (2012) (below) in place of the 4 time series figures. This would be easier for the reader to interpret. This would greatly reduce the number of words in the section and make the overall microphysical picture clearer. There are just too many small, insignificant details stated for me to try and see what the overall picture of each case is.

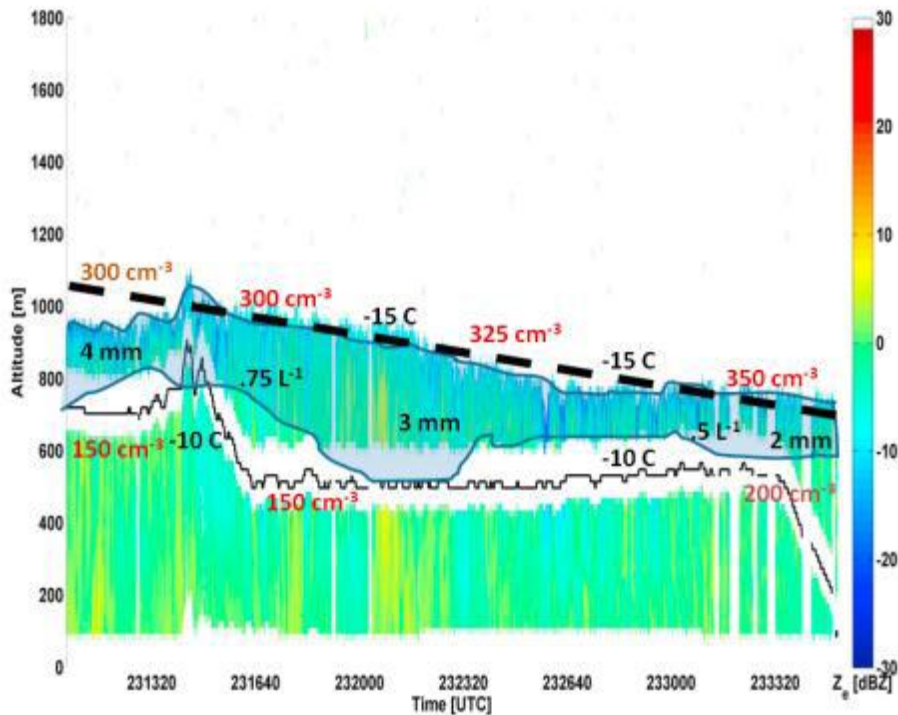


Figure 9. Vertical cross section of Z_e from the W-band radar for a cloud deck observed on the second flight of April 8. The blue shaded regions denote the approximate location of the liquid layer derived from the in situ profiles of LWC . Maroon values denote PCASP concentration measured above and below cloud, black values in mm are median mass diameter of ice crystals, and values in L^{-1} denote $N_{ice}(D > 50 \mu m)$. Values in $^{\circ}C$ denote temperature. The solid black line denotes flight track altitude. The dashed black line denotes the approximate location of the temperature inversion.

These sections have been made more concise, but we feel some description of the microphysical structure during a single profile is useful. The beginning of each case now includes a description of the overall structure of the stratocumulus cloud layers, in an attempt to make it much clearer to the reader. The sections describing the microphysics have also been shortened where possible, with the detail about measurements from each probe (e.g LWC , IWC , N_{ice} , N_{drop}).

We will remove the further profile descriptions from the Appendix and include these in the supplementary material.

Line 14-18: I think it would be better to state the variation in predicted IN in your Table rather than what Grosvenor et al. (2012) stated.

We have calculated the uncertainty in the Grosvenor IN predictions for regions not influenced by secondary and included them in the table.

Line 8, 28777: New paragraph.

New paragraph inserted.

Line 22-23, 28777: These rapid fluctuations can also be due to noise from inadequate sampling statistics. In particular, for your larger dendrites, there may only be 4 or less dendrites being sampled per second, which makes this sampling error to be $1/\sqrt{4} = 50\%$

just due to the low number of particles being sampled. You should really be quoting the 0.1 Hz observations when talking about variability in cloud properties for this reason, as the uncertainty due to sampling statistics is likely to be a lot less when the averaging interval is increased.

The number of peak value figures has been reduced, but the sampling error is likely to be acceptable for the regions of secondary ice production where counts are higher, so some of these have been kept. The lines here also refer to transitions from one state to the other, for example predominantly liquid conditions very quickly replaced by glaciated cloud due to the HM process. This is distinct from repeated fluctuations in the 1Hz data that may be subject to significant error due to poor counting statistics.

Paragraph at line 25, 28779: This discussion needs to be expanded factoring in the relative impact of the three aerosol indirect effects in determining the microphysical properties of these clouds. The same follows for the following paragraph comparing your observations against the Grosvenor study.

The importance of each hypothesis has now been included in the discussion section. (*line 483-488;600-603;615-617*). We have also added a new conclusion based on the possibility that the riming indirect effect played a role in reducing ice water contents in the spring case with higher aerosol loadings.

Interactive comment on “Observations and comparisons of cloud microphysical properties in spring and summertime Arctic stratocumulus during the ACCACIA campaign” by G. Lloyd et al.

Anonymous Referee #2

Received and published: 5 January 2015

This paper reports on some interesting microphysical observations from a set of flights during spring and summer through arctic stratocumulus near Svalbard. The authors point out that few in-situ measurements of ice and aerosol have been made in arctic stratocumulus and this is still largely true. However, the measurements that have been made over the years are tending to converge (see Morrison et al., 2011, Nature Geo-science). The authors note substantial seasonal differences in the microphysical, and glaciation, of mixed-phase arctic clouds. The observed summertime clouds appear to be more heterogeneous with pockets of ice formed apparently by rime splintering. Spring-time clouds generally had lower ice concentrations than summer. Comparisons of the observed ice concentrations with predictions using the Demott et al. (2010, PNAS) were also discussed in the paper. I found the paper easy to read and the observations are quite interesting.

While I generally find the paper to be a useful contribution to the literature on the measured microphysical properties of arctic mixed-phase stratocumulus, I also think that the paper is missing some elements, I list them below.

(1) I think the paper needs a section that provides some meteorological context for the cloud cases and the observations. Since the larger scale synoptic flow can set the stage for a given

microphysical response of the cloud system to aerosol/IN, providing an overview of the general flow along with the vertical thermal and moisture structure would be very helpful.

We have added or improved upon the description of the synoptic conditions at the start of each case description. This aims to provide some context to the large-scale forcing in the region. We have looked at the vertical thermal and moisture structure. Fig. 11 for example shows the temperature profile of the atmosphere measured by the aircraft. When looking at dew points these showed a marked dry layers above the cloud in the inversion layer. We haven't presented this in any new figure. We have mentioned this dry layer in relation to dew point measurements (*lines 491-494*)

(2) The authors do a very nice job of comparing their results to results from an Antarctic study. I think the paper would be enriched if the authors could cast their results in the context of the other papers published on ice concentrations/IN in arctic clouds. For in-stance, Rangno and Hobbs published a paper in 2001 (J. Geophys. Res., pg 15,065) in which they also discuss the importance of rime-splintering for high ice concentrations in arctic mixed-phase stratocumulus. In addition to pointing out that there is no clear temperature dependence to ice concentrations in arctic clouds, Rangno and Hobbs also indicated that a possible threshold droplet size exists that relates to maximum ice concentration. Do your observations show similar results? Other articles have dis-cussed ice concentrations and the vertical thermal structure of the atmosphere (Curry et al., 1997, JGR; Pinto, 1998, JAS; Rogers et al., 2001; JGR; Prenni et al., 2007; etc.); results from these papers may help place your results into a broader context.

Although we haven't done habit classification on our 2D-S dataset from looking at the images we generally observed that columnar crystals dominated the imagery, despite the presence of some less pristine ice that could simply be described as irregular. For this reason we believe the enhanced concentrations in the spring cases was very likely due to secondary ice production through rime-splintering. In the manuscript the presence of temperature inversions has been discussed, as this is a common finding at the top of stratocumulus cloud layers in this region. During the spring cases these inversions were stronger and interestingly the cloud penetrated some distance into the inversion layer.

We have added a paragraph discussing the Rangno and Hobbs (2001) and the relevance of their work to our results. (*lines 586-598*)

Rogers et al. (2001) found similar ice concentrations and evidence for a few IN in stratus clouds they studied. Their findings are consistent with the cases presented in this paper. A sentence has been added to describe this in the discussion. (*lines 581-583*)

(3) As I understand it, the IN parameterization of Demott provides an estimate of the local (in space) ice concentration based on temperature and the number of aerosol beyond a certain size. However, the ice concentration measured in clouds is a conse-quence of not only local ice nucleation processes, but also of convergence and diver- gence due to vertical sedimentation and advection. Since not all ice particles grow at the same rate, one might

imagine larger ice particles, for example, sedimenting away from a nucleation zone and therefore leading to a lower measured ice concentration. I wonder if these sorts of effects are important or if they are negligible.

These processes can change the concentrations of the crystals observed. We have noted this in paper. However, the range of crystal concentrations observed can be explained by the uncertainty in the DeMott parameterisation discussed below.

(4) In Demott's paper, the observed data are quite scattered about the 1:1 line in comparison to the parameterization. For your observed cases, does the scatter in the points shown in Fig.3b cover the range of your observed ice concentrations? For instance, your case 1c produces IN concentrations of 1.24 or 2.05 but the scatter in Demott's Fig. 3b indicate that observed IN concentrations at these predicted values can be up to 10 per liter or as low as a few tenths per liter. I'm primarily curious about this because if the ice concentrations sit within the range of scatter Demott shows, it might provide a small amount of evidence that IN could have been responsible for the ice. (Whereas in your rime-splintering observations, this is clearly not the case.)

A section has been added to discuss the variation in the D10 parameterisation and we find that the spread in our ice concentrations is within the variability of the points in fig. 3b of the DeMott et al. (2010) paper.

Interactive comment on “Observations and comparisons of cloud microphysical properties in spring and summertime Arctic stratocumulus during the ACCACIA campaign” by G. Lloyd et al.

A. Kirchgaessner

acrki@bas.ac.uk

Received and published: 25 November 2014

The affiliation for A. Kirchgaessner and T. Lachlan-Cope is not correct. They both are affiliated with the British Antarctic Survey, NERC, High Cross, Madingley Rd, Cambridge CB3 0ET, UK. Thanks.

This affiliation has now been added.

1 Observations and Comparisons of Cloud Microphysical Properties in Spring and
2 Summertime Arctic Stratocumulus during the ACCACIA campaign.

3 G. ~~Lloyd~~Lloyd^{1*}, T.W. ~~Choularton~~Choularton¹, K.N. ~~Bower~~Bower¹, J. ~~Crosier~~Crosier¹, H.
4 ~~Jones~~Jones¹, J. R. ~~Dorsey~~Dorsey¹, M.W. ~~Gallagher~~Gallagher¹, P. ~~Connolly~~Connolly¹, A. C.
5 R. ~~Kirchgaessner~~Kirchgaessner² and T. Lachlan-~~Cope~~Cope².

Formatted: Superscript

6 1. Centre for Atmospheric Science, University of Manchester, UK

7 2. British Antarctic Survey, NERC, High Cross, Madingley Rd, Cambridge CB3 0ET, UK

8 Corresponding author G. Lloyd, Centre for Atmospheric Science, University of Manchester,
9 Oxford Road, Manchester M13 9PL email: gary.lloyd@manchester.ac.uk

10
11
12 **Abstract**

13 Measurements from four case studies in spring and summer-time Arctic stratocumulus clouds
14 during the Aerosol-Cloud Coupling And Climate Interactions in the Arctic (ACCACIA)
15 campaign are presented. We compare microphysics observations between cases and with
16 previous measurements made in the Arctic and Antarctic. During ACCACIA, stratocumulus
17 clouds were observed to consist of liquid at cloud tops, often at distinct temperature
18 inversions. The cloud top regions precipitated low concentrations of ice into the cloud below.
19 During the spring cases median ice number concentrations ($\sim 0.5 \text{ L}^{-1}$) were found to be lower
20 by about a factor of 5 than observations from the summer campaign ($\sim 3 \text{ L}^{-1}$). Cloud layers in
21 the summer spanned a warmer temperature regime than in the spring and enhancement of ice
22 concentrations in these cases was found to be due to secondary ice production through the
23 Hallett-Mossop (H-M) process. Aerosol concentrations during spring ranged from ~ 300 -400

24 cm^{-3} in one case to lower values of $\sim 50\text{-}100 \text{ cm}^{-3}$ in the other. The concentration of aerosol
25 with sizes, $D_p > 0.5 \mu\text{m}$, was used in a primary ice nucleus (IN) prediction scheme, DeMott et
26 al. (2010). Predicted IN values varied depending on aerosol measurement periods, but were
27 generally greater than maximum observed median values of ice crystal concentrations in the
28 spring cases, and less than the observed ice concentrations in the summer due to the influence
29 of secondary ice production. Comparison with recent cloud observations in the Antarctic
30 summer (Grosvenor et al., 2012), reveals lower ice concentrations in Antarctic clouds in
31 comparable seasons. An enhancement of ice crystal number concentrations (when compared
32 with predicted IN numbers) was also found in Antarctic stratocumulus clouds spanning the
33 Hallett-Mossop (H-M) temperature zone, but concentrations were about an order of
34 magnitude lower than those observed in the Arctic summer cases, but were similar to the
35 peak values observed in the colder Arctic spring cases, where the H-M mechanism did not
36 operate.

37 | 38 **1.0 Introduction**

Formatted: Font: Not Bold

39 The Arctic is a region that has experienced rapid climate perturbation in recent decades, with
40 warming rates there being almost twice the global average over the past 100 years (ACIA,
41 2005, IPCC 2007). The most striking consequence of this warming has been the decline in
42 the extent and area of sea ice, especially in the warm season. The lowest sea ice extent and
43 area on record were both observed on 13 September 2012 (Parkinson and Comiso, 2013) and
44 despite some uncertainty, ice-free Arctic summers could become a reality by 2030 (Overland
45 and Wang, 2013). The underlying warming is very likely caused by increasing anthropogenic
46 greenhouse gases and arctic amplification, which is a well-established feature of global
47 climate models (see for example IPCC 5th Assessment Report 2014). However, the details of

48 Arctic climate are complex with interactions between the atmospheric boundary layer, cloud,
49 overlying sea-ice and water leading to a number of feedback mechanisms. These interactions
50 are not well understood due to variability in the spatial and temporal extent of feedback
51 mechanisms, and the fact that those that are included in Global Climate Models (GCMs) may
52 not be accurately parameterised (Callaghan et al., 2011). Clouds play an important role in a
53 number of proposed feedback processes that may be active in the Arctic (Curry et al., 1996;
54 Walsh et al., 2002), Arctic clouds are the dominant factor controlling the surface energy
55 budget, producing a mostly positive forcing throughout the year, apart from a brief cooling
56 period during the middle of summer (Intrieri et al., 2002a). These clouds affect both the long-
57 wave (year-round) and short-wave (summer-only) radiation budgets, and influence turbulent
58 surface exchange. Cloud microphysical influence on cloud radiative properties depends on
59 the amount of condensed water and the size, phase and habit of the cloud particles (Curry et
60 al., 1996). These factors are controlled in part by the Cloud Condensation Nuclei (CCN) and
61 Ice Nuclei (IN) concentrations and properties. ~~Very low aerosol concentrations in the Arctic
62 can result in clouds with properties differing greatly from those at mid-latitudes (Tjernström
63 et al., 2008).~~

64 The impact of CCN and IN on cloud properties is significant. A number of hypothesis explain
65 how variation in the availability of CCN and IN may go on to alter microphysical structure.
66 Firstly the thermodynamic indirect effect describes how an increase in CCN leads to a
67 reduction in droplet size, inhibiting the development of drizzle needed for rime-splintering,
68 reducing the efficiency of the process, which may have a significant impact on cloud
69 glaciation around -5 °C. Secondly the glaciation indirect effect states that an increase in IN
70 leads to an increase in the number of ice crystals. Finally the riming indirect effect inhibits
71 ice mass growth as increasing CCN leads to smaller drops with lower collection efficiencies
72 that reduces the riming rate (Lohmann and Feichter, 2005).

73 In relation to these 3 hypotheses there have been a range of results presented in the literature
74 in recent years investigating the impact of aerosol on arctic clouds. For example Lance et al.
75 (2011) presented aircraft data from the arctic mixed phase clouds gathered in the Alaska
76 region from the Aerosol, Radiation, and Cloud Processes affecting Arctic Climate
77 (ARCPAC) experiment. They reported that the concentration of ice particles greater than 400
78 µm is correlated with the concentration of droplets larger than 30 µm, providing support for
79 the riming indirect effect. They found that mixed phase clouds in polluted conditions with a
80 high aerosol population due to long range transported biomass burning aerosol contained a
81 narrower droplet size distribution and 1-2 orders of magnitude fewer precipitating ice
82 particles than clean clouds at the same temperature. Although this finding isn't consistent
83 with the glaciation indirect it is likely due to the increase in aerosol not providing active IN in
84 clouds over the temperature range that was investigated.

85 Jackson et al. (2012) presented data from the Indirect and Semi-Direct Aerosol Campaign
86 (ISDAC) and from the Mixed-Phase Arctic Cloud Experiment. They found no evidence for a
87 riming indirect effect but did find a correlation between ice crystal number concentration and
88 above cloud aerosol concentration in this case. This finding, together with sub-adiabatic
89 liquid water contents suggested that ice nuclei were being entrained from above cloud top in
90 their studies , which is consistent with the glaciation indirect effect. They also reported lower
91 ice crystal number concentrations and lower effective radius in more polluted cases compared
92 to data collected in cleaner single-layer stratocumulus conditions during The Mixed-Phase
93 Arctic Cloud Experiment (M-PACE)(Verlinde et al., 2007), which is consistent with the
94 operation of the thermodynamic indirect effect. They concluded that a wider range of arctic
95 clouds need to be studied to investigate the generality of their results.

96 A paucity of observations in the Arctic means that neither the aerosol processes, nor cloud
97 properties are well understood or accurately represented within models, with the result that

98 aerosol and cloud-forcing of Arctic climate is poorly constrained. - An important aspect of
99 modelling arctic clouds is the use of primary IN parameterisations to initiate the ice phase in
100 these clouds. The measurements made in this study of both aerosol properties and ice number
101 concentrations allowed us to compare predicted ice nuclei concentrations from the DeMott et
102 al. (2010) IN parameterisation and cloud ice concentrations measured by microphysics
103 probes.

104 In the Arctic lower troposphere low cloud dominates the variability in Arctic cloud cover
105 (Curry et al., 1996), with temperature and humidity profiles showing a high frequency of one
106 or more temperature inversions (Kahl, 1990) below which stratocumulus clouds form. During
107 the Arctic summer, therefore, these low clouds often consist of multiple layers, with a
108 number of theories describing their vertical separation (Herman and Goody, 1976; Tsay and
109 Jayaweera, 1984; McInnes and Curry, 1995a). Such cloud layers have been observed during
110 different seasons but the relationship between temperature and the formation of ice in them is
111 not well understood. Jayaweera and Ohtake (1973) observed very little ice above $-20\text{ }^{\circ}\text{C}$, but
112 Curry et al. (1997) observed ice to be present in clouds at temperatures between $-8\text{ }^{\circ}\text{C} < T < -$
113 $14\text{ }^{\circ}\text{C}$ during the Beaufort Arctic Storms Experiment (BASE). It is possible that the large
114 variation in temperature at which glaciation is observed is caused by changes in the
115 concentration and composition of aerosol (Curry, 1995). Recent work, such as in the Arctic
116 Cloud Experiment (ACE) (Uttal et al., 2002) has improved our knowledge of Arctic mixed-
117 phase clouds, which dominate in the coldest 9 months of the Arctic year. ACE reported that
118 clouds were mainly comprised of liquid tops, tended to be very long lived and continually
119 precipitated ice. The longevity of these clouds might be considered unusual as the formation
120 of ice leads to loss of water through the Wegener-Bergeron-Findeison process. More recently
121 the ~~Mixed Phase Arctic Cloud Experiment (M-PACE, 2004)~~ investigated the Arctic autumn
122 transition season. ~~M-PACE was conducted~~ on the North slope of Alaska, in the area to the

123 east of Barrow (~~Verlinde et al., 2007~~). Again predominantly mixed-phase clouds were
124 observed with liquid layers present at temperatures as low as -30 °C. ~~Remote sensing studies~~
125 ~~also showed that ice was generally present in low concentrations, mostly associated with~~
126 ~~precipitation shafts, however, there was also evidence of light snow below thicker layer~~
127 ~~clouds. IN concentrations were also measured and observed to be low, consistent with liquid~~
128 ~~water being observed down to very low temperatures.~~ Here we present detailed airborne
129 microphysical and aerosol measurements made in stratocumulus cloud regions in the
130 European Arctic during the recent Aerosol-Cloud Coupling And Climate Interactions in the
131 Arctic (ACCACIA) campaigns. We present data from two aircraft during early spring, in
132 March and April 2013, and from a single aircraft during the following Arctic summer, in July
133 2013.

134 The objectives of this paper are:

- 135 1. To report the microphysics and cloud particle properties of Arctic clouds, and the
136 properties, number and size distributions of aerosols in the vicinity of these
- 137 2. To identify the origin of the ice phase in these clouds and to compare ice crystal
138 number concentrations with the parameterisation of primary Ice Nucleus (IN)
139 concentrations of DeMott et al. (2010)).
- 140 3. To compare the cloud physics in spring and summer conditions and to identify any
141 contributions of secondary ice particle production.
- 142 4. To compare and contrast the mixed phase cloud microphysics of Arctic clouds with
143 clouds observed in the Antarctic.

144
145 **2.0 Methodology**

146 The ACCACIA campaigns took place during March-April 2013 and July 2013. They were
147 conducted in the region between Greenland and Norway mainly in the vicinity of Svalbard
148 ~~(and further afield to the south and west of the archipelago).~~ The overarching theme of the
149 project was to reduce the large uncertainty in the effects of aerosols and clouds on the Arctic
150 surface energy balance and climate. Key to the work presented here is an understanding the
151 microphysical properties of Arctic clouds and their dependence on aerosol properties. To this
152 end the FAAM BAe-146 aircraft performed a number flights incorporating profiled ascents,
153 descents and constant altitude runs below, within and above cloud during the spring period.
154 This provided high-resolution measurements of the vertical structure of the cloud
155 microphysics and the aerosol properties in and out of cloud regions. The British Antarctic
156 Survey (BAS) Twin Otter aircraft flew during both campaign periods, providing a subset of
157 the BAe-146 measurements. It was the only aircraft present during the summer period. A
158 total of 9 science flights were conducted during the spring period with complementary flights
159 from the BAS twin otter and 6 flights by the BAS twin otter alone during the summer period.

160 Two case studies are selected from both the early spring and summer campaigns. The spring
161 campaign case studies were selected for having quite different aerosol loadings within the
162 boundary layer. One was in relatively clean Arctic air with low total aerosol numbers, while
163 the second had higher aerosol loadings in the boundary layer. Summer flight cases were
164 selected for being the cases with higher cloud layer temperatures in ~~comparison to the spring~~
165 ~~cases. Summer case cloud layer temperatures were significantly higher than in the spring~~
166 ~~cases, and were observed to be in the temperature zone, -3°C to -9°C , where a powerful~~
167 ~~mechanism of range suitable for~~ secondary ice ~~partiele~~ production through ~~rime splintering,~~
168 the Hallett-Mossop ~~mechansim, (H-M)Process~~ (Hallett and Mossop, 1974,) to take place.
169 This process is known to operate under particular conditions, and so could greatly enhance
170 ice crystal number concentrations. Temperature profiles in the spring cases revealed

171 stratocumulus cloud temperatures generally between $-10\text{ }^{\circ}\text{C} < T < -20\text{ }^{\circ}\text{C}$, outside of the H-
172 M zone.

173

174 **2.1 Instrumentation**

Formatted: Font: Not Bold, English (U.S.)

175 Instrumentation onboard the Facility for Airborne Atmospheric Measurements (FAAM)
176 British Aerospace-146 (BAe-146, or 146) aircraft used for making measurements of the cloud
177 and aerosol microphysics reported in this paper included: the Cloud Imaging Probe models
178 15 and 100 (CIP-15 and CIP-100, Droplet Measurement Technologies (DMT), Boulder,
179 USA) (Baumgardner et al., 2001), the Cloud Droplet Probe (CDP-100 Version 2, DMT)
180 (Lance et al., 2010) and the Two Dimensional-Stereoscopic Probe (2D-S, Stratton Park
181 Engineering Company Inc. Boulder, USA) (Lawson et al., 2006). The CIP-15 and CIP-100
182 are optical array shadow probes consisting of 64 element photodiode arrays providing image
183 resolutions of $15\text{ }\mu\text{m}$ and $100\text{ }\mu\text{m}$ respectively. The 2D-S is a higher resolution optical array
184 shadow probe which consists of a 128 element photodiode array with image resolution of 10
185 μm . The CDP measures the liquid droplet size distribution over the particle size range $3 < d_p$
186 $< 50\text{ }\mu\text{m}$. The intensity of forward scattered laser light in the range $4\text{-}12^{\circ}$ is collected and
187 particle diameter calculated from this information using Mie scattering solutions (Lance et
188 al., 2010).

189

190 A Cloud Aerosol Spectrometer (CAS, DMT) and a Passive Cavity Aerosol Spectrometer
191 Probe (PCASP-100X, DMT) were both used to measure aerosol size distributions onboard
192 the 146. The CAS measures particles in the size range $0.51 < d_p < 50\text{ }\mu\text{m}$ using forward
193 scattered light from single particles in the $4\text{-}13^{\circ}$ range and backscattered light in the $5\text{-}13^{\circ}$

194 range. Particle size can be determined from both the forward and back-scattered light
195 intensity using Mie scattering solutions (Baumgardner et al., 2001). The PCASP is another
196 Optical Particle Counter (OPC) and measures aerosol particles in the size range $0.1 < d_p < 3$
197 μm . In this instrument, particles are sized through measurement of the intensity of laser light
198 scattered within the $35\text{-}120^\circ$ range (Rosenberg et al., 2012). All the above instruments were
199 mounted externally on the FAAM aircraft. ~~Non-refractory aerosol composition measurements~~
200 ~~were provided using an Aerodyne Compact Time of Flight Aerosol Mass Spectrometer (C-~~
201 ~~ToF-AMS) whilst aerosol black carbon measurements were provided by a single particle soot~~
202 ~~photometer (SP-2, DMT).~~ Results from these will be reported elsewhere. Examples of
203 additional core data measurements that were also used in this paper include temperature
204 (Rosemount/Goodrich type 102 temperature sensors) and altitude measured by the GPS-aided
205 Inertial Navigation system (GIN).

206
207 Instrumentation on board the Twin Otter Meteorological Airborne Science Instrumentation
208 (MASIN) aircraft, relevant to measurements reported in this paper included: A CDP-100 for
209 drop size distributions; a 2D-S (summer only), both similar to those on the FAAM aircraft; a
210 CIP-25 (as on FAAM except consisting of a 64 element photodiode array providing an image
211 resolution of $25 \mu\text{m}$) and core data including temperature -measured by Goodrich Rosemount
212 Probes (models; 102E4AL and 102AU1AG for non-deiced, and a de-iced temperatures
213 respectively, similar to those used on the FAAM aircraft) and altitude derived from the
214 aircraft avionics (Litef AHRS) system.

Formatted: English (U.S.)

216 **2.2 Data Analysis**

Formatted: Font: Not Bold, English (U.S.)

217 During each science flight measurements of aerosol and cloud microphysical properties were
218 made. The techniques used to interpret these data are described below.

219

220 **Cloud Microphysics Measurements**

221 In the paper, 1Hz data from all cloud and aerosol instruments have been further averaged
222 over 10 second periods for presentation ~~unless peak values, from the 1Hz data are used, as~~
223 ~~stated. The different flight profiles and straight and level aerosol and cloud sampling runs for~~
224 ~~all cases are summarised in Table 1. A main focus of this study is the formation of the ice~~
225 ~~phase in arctic stratocumulus.~~ Measurements from the 2D-S probe have been presented in
226 preference to other 2D probe data due this probes significantly faster response time (by > a
227 factor of 10), and greater resolution. When comparing CIP-15 and 2D-S size distributions we
228 found good agreement over their respective size ranges. During the spring cases it was
229 possible to combine 2D-S data with measurements from the CIP-100 to extend the cloud
230 particle size range. Analysis of imagery from these Optical Array Probes (OAPs) was used to
231 calculate number concentrations and discriminate particle phase. Identification of irregular
232 particles, assumed to be ice, was achieved through examination of each particles circularity
233 (Crosier et al., 2011). Ice Water Contents (IWCs) were determined using the Brown and
234 Francis (1995) mass dimensional relationship. This mass dimensional relationship is widely
235 used in the literature for mixed phase cloud (e.g. Crosier et al. 2011). Baker and Lawson
236 (2006) found discrepancies between their treatments of data using habit recognition and the
237 Brown and Francis scheme. In our case studies where the IWC is high most of the mass is
238 dominated by small ice crystals, in which good agreement is found between the Brown and
239 Francis and Baker and Lawson.

240 All cloud microphysics probes were fitted with “anti-shatter” tips (Korolev et al.,
241 [2011; Korolev et al. 2013](#)) to mitigate particle shattering on the probe. However, even with
242 these modifications shattering artifacts may still be present, particularly under some cloud
243 conditions and these need to be corrected for (Field et al. 2006). To minimise such artifacts,
244 Inter-Arrival Time (IAT) histograms were analysed in an attempt to identify and remove
245 these additional particles, i.e. by removing particles with very short IATs that are indicative
246 of shattered ice crystals. Crosier et al. (2013) reported that careful analysis of IAT histograms
247 for different cloud microphysical conditions is needed to determine the most appropriate IAT
248 threshold for best case elimination of such artifacts. For example, in regions of naturally high
249 ice crystal number concentrations, such as in the H-M secondary ice production temperature
250 zone, the minimum IAT threshold may need to be reduced more than is usual so as not to
251 exclude too many naturally generated ice crystals with short IATs. In this study, we found a
252 minimum IAT threshold of 1×10^{-5} s and 2×10^{-5} s for the 2D-S and CIP-15 instruments
253 respectively, to be appropriate IAT values for the majority of cloud region data presented.

254 It was found that the CIP probes and 2D-S ice crystal number concentrations differed by less
255 than 20% over their common size range. In this paper we present the data from the 2D-S due
256 to its larger size range, higher resolution and faster response time.

~~257 Measurements of the liquid and ice properties of cloud layers observed during each science
258 flight were binned as a function of altitude and are presented in figures 10, 11 and 12. The
259 case descriptions provide descriptions of typical cloud penetrations by the aircraft and
260 describe the dominant microphysical structures observed during each science flight.
261 Additional descriptions of profiles made during each flight can be found in the Appendix~~

263 2.4. Aerosol Measurements

264 ~~¶~~We did not directly measure IN concentrations during each flight, however information in
265 each case study, about aerosol concentration ~~measurements were~~and size was used to
266 calculate the predicted primary ice nuclei (IN) concentrations from the DeMott et al. (2010,
267 hereafter *D10*) parameterisation of primary ice nuclei numbers, which is dependent on the
268 number concentration of aerosol particles with diameters $> 0.5 \mu\text{m}$. Combined measurements
269 of the aerosol concentration using the PCASP and CAS (for spring), and CAS (for summer),
270 were used from cloud free regions selected by applying maximum Relative Humidity (RH)
271 thresholds. This was done to reduce the contribution of any haze aerosol particles less than
272 $0.5 \mu\text{m}$ in size growing into the size range at higher humidities and being incorrectly
273 included. The FAAM CAS instrument has a lower size threshold of $0.51 \mu\text{m}$. *D10* notes that
274 the maximum possible aerosol size that could be measured and included in their *D10*
275 parameterization was $1.6 \mu\text{m}$. However, due to the size bins utilised by the CAS instrument
276 this upper threshold had to be relaxed to $2 \mu\text{m}$, although the extra contribution to the aerosol
277 concentrations used in the calculations is likely to be small. ~~Grosvenor et al. (2012)~~
278 ~~demonstrated that the scheme is not particularly sensitive to small changes in total aerosol~~
279 ~~concentrations $> 0.5 \mu\text{m}$ in clean Antarctic regions.~~ Measurements from the higher resolution
280 PCASP were selected from the size range $0.5 \mu\text{m}$ to $1.6 \mu\text{m}$, in keeping with the *D10* scheme.
281 The *D10* predicted IN concentrations were then compared directly as a function of
282 temperature with the observed ice crystal concentrations. The minimum observed median
283 temperature was input to *D10* and predicted IN numbers compared with the maximum
284 observed median ice crystal number concentrations (Fig. 11) for the clouds during each of the
285 4 cases. The results are shown in Table 2.

286 The results of this comparison from all 4 cases can be compared with previous observations
287 of Arctic clouds and with recent aircraft measurements of clouds over the Antarctic Peninsula
288 in the summer (Grosvenor et al., 2012).

289

290 3.0 Spring Case 1 - Friday 22 March 2013 (FAAM flight B761)

291 ~~On this day the~~The FAAM aircraft ~~first~~ flew from Kiruna, Sweden (67.85°N, 20.21°E) to
292 Svalbard, Norway landing at Longyearbyen, (78.22°N, 15.65°E) to refuel. After take-off at ~
293 1145 UTC a ~ 2 hour science flight was undertaken to the south east of Svalbard (Fig. 1)
294 before returning to Kiruna. The objective was to investigate stratocumulus cloud in this area,
295 ~~near to the ice edge, and from over ice to open ocean (moving from N to S in the target area).~~
296 The flight focused on a series of profiled descents and ascents to enable measurements to be
297 made of the cloud layer from below cloud base to above cloud top and into the inversion
298 layer above. During the flight there were 3 significant penetrations through the inversion at
299 cloud top and in each case there was a marked temperature increase of ~~~5°C~~ 5°C.

300 Microphysical time series data for this case are presented, with the relevant runs highlighted
301 in Figure 2. A description of one cloud profile is given here, with further profiles described in
302 ~~Appendix A. For this case, boundary~~ the supplement.

303 Boundary layer aerosol number concentrations (from the PCASP) were found to be relatively
304 low at ~ 50-100 cm⁻³. ~~Widespread~~ A blocking high pressure system East of Greenland was
305 present, with a trough over eastern Scandinavia. The area of operation was situated on the
306 north eastern side of the anticyclone with widespread low cloud ~~was~~ observed south and east
307 of Svalbard (Fig. 1), with winds from the north advecting from over the sea-ice towards
308 open sea. Earlier dropsonde measurements (on the transit into Longyearbyen prior to
309 refuelling) showed surface winds of ~ 3 m s⁻¹ increasing to 15 m s⁻¹ at 500 mb. The cloud
310 layers during this flight were found to contain generally uniform liquid water content profiles,
311 which were found to be approximately adiabatic. The clouds were situated over the

312 temperature range $-15\text{ }^{\circ}\text{C} < T < -20\text{ }^{\circ}\text{C}$. Generally low concentrations of ice, often in isolated
313 pockets, were observed in these clouds.

314

315

316 **3.1 Profiled Descent A1**

317 During profile A1 the aircraft (now travelling north) descended from the inversion layer.

318 Cloud top was encountered at 1650 m ($T = -18.6\text{ }^{\circ}\text{C}$). The highest values of N_{ice} were

319 observed in the cloud top region, at $\sim 4\text{ L}^{-1}$ ~~with peaks up to 7 L^{-1} where IWCs were 0.15 g m^{-3}~~

320 ~~m^{-3} . Particles here consisted of small irregular ice particles (mean size $\sim 360\text{ }\mu\text{m}$) that showed~~

321 evidence of riming, together with small droplets. ~~CDP~~ LWC at cloud top increased to 0.3 g

322 m^{-3} with $N_{drop} \sim 55\text{ cm}^{-3}$ (mean diameter $\sim 17\text{ }\mu\text{m}$). ~~At an altitude of around 1400 m as~~ As the

323 aircraft descended ($\sim 250\text{ m}$ below cloud top) N_{ice} decreased to $\sim 1\text{ L}^{-1}$, ~~and~~ while mean ice

324 particle size increased to $\sim 395\text{ }\mu\text{m}$. N_{drop} increased to $\sim 70\text{ cm}^{-3}$, while mean size decreased

325 slightly ($\sim 16\text{ }\mu\text{m}$). ~~), while~~ LWCs generally decreased somewhat to $\sim 0.2\text{ g m}^{-3}$. In spring

326 cases this pattern of steadily reducing LWC with an increase in droplet number towards cloud

327 base was frequently observed (Fig. 10). As the aircraft descended to an altitude of $\sim 1150\text{ m}$,

328 N_{ice} increased by approximately a factor of 2 (to $\sim 2\text{ L}^{-1}$). At around 1315 UTC a number of

329 rapid transitions from liquid to predominantly glaciated conditions were observed in the mid

330 cloud region at 730 m and $T = -12\text{ }^{\circ}\text{C}$. ~~The initial phase change occurred as LWC decreased~~

331 ~~from 0.2 to 0.01 g m^{-3} while IWCs increased to a peak value of 0.2 g m^{-3} and peak N_{drop} fell~~

332 ~~close to 1 cm^{-3} .~~ 2D-S imagery (Fig 3c.) highlights these changes taking place as small

333 droplets are quickly replaced by small irregular ice crystals and eventually larger snow

334 particles (mean diameter $\sim 610\text{ }\mu\text{m}$) that consisted of heavily rimed ice crystals and

335 aggregates, some of which can be identified as exhibiting a dendritic habit. Observations of

336 ~~dendritic ice are consistent with the ice crystal growth habit expected at this temperature level~~
337 ~~(-12 °C).~~ Three further swift phase transitions were observed as the aircraft approached cloud
338 base. LWC in the liquid dominated regions was between ~ 0.15 and 0.25 g m^{-3} while N_{drop}
339 peaked at $\sim 130 \text{ cm}^{-3}$. During the ice phase sections of the transition cycle, mean particle
340 sizes were $\sim 615 \text{ }\mu\text{m}$ and N_{ice} ~~peaked at up to 5 L^{-1} . was a few per litre.~~ The contribution of
341 these glaciated cloud regions to the IWC was considerable, with values ~~up to around~~ 0.1 g m^{-3}
342 recorded. These transitions ended as the aircraft descended below cloud base ($T = -12 \text{ }^\circ\text{C}$) at
343 700 m asl, and precipitating snow was observed (mean size $\sim 710 \text{ }\mu\text{m}$). Measurements of the
344 ice phase during spring cases often showed increasing ice crystal size towards cloud base,
345 with the largest ice particles measured in precipitation from the cloud layers above.

348 **4.0 Spring Case 2 – Wednesday 3 April 2013 (FAAM flight B768)**

349 The FAAM aircraft departed Longyearbyen at around 11 UTC and conducted measurements
350 to the NW of Svalbard to investigate low-level clouds over ~~sea ice as well as the transition to~~
351 ~~deeper more convective type cloud as the aircraft moved away from the ice edge and over~~
352 ~~warmer water~~ the sea ice (moving from NW to SE in the target area - Fig 1). A low pressure
353 (1004 mb) region was centred south of Svalbard with an associated band of cloud and
354 precipitation. To the NW of Svalbard, within the measurement area, surface winds were E-
355 NE and $< 10 \text{ m s}^{-1}$. Measurements revealed an air mass containing significantly more aerosol
356 than in Spring case 1, with PCASP concentrations typically $\sim 300\text{-}400 \text{ cm}^{-3}$ in the boundary
357 layer. During the flight the aircraft made two distinct saw tooth profiles through the cloud
358 layer and into the inversion above cloud top where temperatures in each instance increased by
359 $\sim 2^\circ\text{C}$. Figure 4 shows time series of the microphysical measurements made during this

360 science flight. Further profile descriptions can be found in Appendix B the supplementary
361 material. Despite the contrast in aerosol loadings when compared with the first spring case,
362 where aerosol concentrations were much lower, the cloud layers were similar with generally
363 uniform structure and low concentrations of primary ice. Despite the cloud layers being
364 situated in slightly higher temperatures ($-12\text{ }^{\circ}\text{C} < T < -16\text{ }^{\circ}\text{C}$) the concentrations of ice was
365 similar to spring case 1.

366

367 **4.1 Profiled Descent B1**

368 Flying NW, the aircraft performed a profiled descent from the inversion layer ($T = -16.5\text{ }^{\circ}\text{C}$)
369 into cloud top, $\sim 1550\text{ m}$ asl, where the measured temperature was $-17\text{ }^{\circ}\text{C}$. LWCs rose to ~~a~~
370 ~~peak value of~~ $\sim 0.9\text{ g m}^{-3}$ and N_{drop} (mean diameter $\sim 15\text{ }\mu\text{m}$) peaked at $\sim 320\text{ cm}^{-3}$. The
371 highest values of N_{ice} never exceeded 0.5 L^{-1} in this cloud top region and imagery from the
372 2D-S probe revealed many small droplets with isolated small (mean size $\sim 223\text{ }\mu\text{m}$) irregular
373 ice crystals (Fig 5a). After descending through this brief cloud top region N_{ice} increased to \sim
374 0.5 L^{-1} . As the aircraft descended over the next 500 m mean droplet concentrations gradually
375 increased from 300 cm^{-3} to 370 cm^{-3} with mean diameters decreasing slightly to $12.5\text{ }\mu\text{m}$.
376 LWCs fell from 0.7 g m^{-3} to 0.2 g m^{-3} over the same period ~~and temperatures increased from~~
377 ~~$17.5\text{ }^{\circ}\text{C}$ to $13.5\text{ }^{\circ}\text{C}$.~~ a pattern consistent with spring case 1. N_{ice} values remained fairly
378 constant and IWCs ~~peaked around~~ ~~were~~ $\leq 0.502\text{ g m}^{-3}$. 2D-S imagery showed ice crystals
379 (mean diameter $295\text{ }\mu\text{m}$) to be mainly dendritic in nature. During the last 160 m depth of the
380 cloud before cloud base, N_{ice} remained similar to the mid-cloud region. However,
381 concentrations of liquid droplets measured by the CDP showed greater variability. Peaks in
382 number concentrations reached as high as 430 cm^{-3} , with rapid changes down to as low as
383 110 cm^{-3} .

384 The aircraft passed cloud base at 700 m asl encountering low concentrations ($< 0.5 \text{ L}^{-1}$) of
385 precipitating snow. Interestingly, as the aircraft continued its descent (to 50 m asl) a
386 significant increase in N_{ice} was observed ($T = -9^\circ\text{C}$), with 10 second mean values of 2 L^{-1} and
387 ~~1 second peak values of 4 L^{-1}~~ . Images from the 2D-S revealed (fig. 5d) snow precipitation
388 co-existing with small columnar ice crystals. CDP LWC was very low, $< 0.01 \text{ g m}^{-3}$, however
389 examination of the 2D-S imagery showed the presence of spherical drizzle droplets, larger
390 than the maximum detectable size of the CDP. Size distribution data from the 2D-S in this
391 region revealed an additional mode dominated by these smaller columnar ice crystals,
392 typically $80 \mu\text{m}$ in size. As the aircraft ascended again, these higher concentrations of ice
393 crystals diminished ~~before cloud base was reached again at $\sim 850\text{m asl}$.~~

394

395

396 **5.0 Summer Case 1 – Tuesday 18th July 2013 (Flight number M191)**

Formatted: Font: Not Bold

397 The BAS Twin Otter aircraft departed Longyearbyen airport at ~ 07 UTC to conduct a ~ 2 hr
398 science flight to the North of Svalbard (Fig. 1). Examination of surface pressure charts
399 showed a slack low pressure around Svalbard, with an occluded front to the East. Extensive
400 low cloud was present in the area with light winds $< 5 \text{ m s}^{-1}$ from the North. The objectives of
401 the flight were to measure aerosol concentrations and composition in the vicinity of cloud,
402 together with the microphysical properties of the clouds by undertaking a combination of
403 profiles and straight and level runs through stratocumulus cloud layers to capture the
404 microphysical structure. Time series of data collected during this flight are presented in figure
405 6. Profile C2 is described below, with details of the measurements made during C1 found in
406 Appendix C the supplement. Cloud layers during this case were found to be situated in the H-
407 M temperature zone with greater variability in microphysical structure when compared with

408 the spring cases. At cloud top ice concentrations were found to be similar to the spring cases.
409 However at times in the body of the cloud secondary ice production would cause significant
410 areas of glaciated cloud, which appeared to lead to greater variability in the liquid water
411 profile of the clouds when compared to the colder layers observed in the spring.

412

413 **5.1 Profile C2**

Formatted: Font: Not Bold, English (U.K.)

414 The aircraft performed a sawtooth profile, descending from cloud top at ~ 3300 m down to a
415 minimum altitude of ~ 2300 m followed by a profiled ascent to complete the sawtooth .

416 During the descent into cloud top ($T = -9^{\circ}\text{C}$) LWCs rose sharply to peak values of 0.3 g m^{-3}

417 and N_{drop} (mean diameter $19 \mu\text{m}$) increased to 155 cm^{-3} . N_{ice} in the cloud top regions peaked

418 at 1 L^{-1} . With decreasing altitude, LWC declined gradually to values close to 0.01 g m^{-3} . As

419 the temperature increased to above -8°C , ice crystal number concentrations (mean diameter

420 $210 \mu\text{m}$) increased to 5 L^{-1} , with peaks to $\sim 12 \text{ L}^{-1}$. 2D-S imagery revealed the presence of

421 small columnar ice crystals together with small liquid droplets (CDP mean diameter $8.5 \mu\text{m}$)

422 and some irregular ice particles. Low concentrations of ice at cloud top was consistent in both

423 summer cases, with periods of enhanced concentrations due to rime-splintering lower down

424 in the clouds.

425 At 2880 m ($T = -6.5^{\circ}\text{C}$) the cloud dissipated until the next cloud layer was encountered 200

426 m below ($T = -5^{\circ}\text{C}$). In this region CDP LWC and N_{drop} were more variable than in the cloud

427 layer above. Generally LWCs were $< 0.1 \text{ g m}^{-3}$ with peaks in N_{drop} to $\sim 155 \text{ cm}^{-3}$ and

428 transitions between liquid cloud and predominantly glaciated cloud were observed. N_{ice}

429 peaked at 25 L^{-1} and IWCs peaked at 0.15 g m^{-3} . During glaciated periods 2D-S imagery

430 showed many columnar ice crystals, typical of the growth regime at this temperature (~ -5

431 $^{\circ}\text{C}$) and consistent with the enhancement of N_{ice} through the H-M process. ~~The aircraft~~

432 reached its minimum altitude ($T = -3^{\circ}\text{C}$) before beginning a profiled ascent to complete the
433 sawtooth. The cloud microphysics of the lower cloud layer were the same as encountered in
434 the descent leg, but with LWCs at times higher (peaks up to 0.2 g m^{-3}). Transitions between
435 liquid and glaciated phases were observed again, with a notable period of high N_{ice} ($T = -4$
436 $^{\circ}\text{C}$), peaking at $\sim 35\text{ L}^{-1}$ and with IWCs as high as 0.3 g m^{-3} . 2D-S images again revealed
437 many columnar ice crystals (mean diameter $295\text{ }\mu\text{m}$), some of which had aggregated, together
438 with irregular ice crystals and liquid droplets. At 2770 m CDP measurements again indicated
439 the presence of a cloud free layer, but over a reduced vertical extent of 100 m , about half the
440 depth observed in the earlier descent. In this region N_{ice} reached 8 L^{-1} in the presence of larger
441 drizzle droplets (fig 7d). Temperatures in the region were around -4°C . Images from the 2D-S
442 showed the presence of small irregular ice crystals with columnar habits. The higher cloud
443 layer cloud base was penetrated at $\sim 2870\text{ m}$, and N_{drop} increased rapidly to 75 cm^{-3} , while
444 LWCs increased gradually to peak values of 0.25 g m^{-3} at cloud top ($T = -6^{\circ}\text{C}$). N_{ice} values
445 were lower than those observed lower in the cloud and generally below 5 L^{-1} . Images of the
446 particles showed the presence of small droplets (CDP mean diameter $18\text{ }\mu\text{m}$) together with
447 small irregular ice crystals (mean diameter $115\text{ }\mu\text{m}$). Greater variation in microphysical
448 structure, with broken cloud layers and transitions between liquid and glaciated phases were
449 evident in the summer cases, which was in contrast to the uniform spring cloud layers.

450

451 **6.0 Summer Case 2 – Wednesday 19 July 2013 (M192)**

Formatted: Font: Not Bold, English (U.S.)

452 The BAS aircraft departed Longyearbyen at $\sim 09\text{ UTC}$ intending to investigate cloud
453 microphysics and aerosol properties to the north of Svalbard (Fig. 1). On arrival in the
454 observation area the forecasted cloud was not present so the flight was diverted to the south
455 east of Svalbard to meet an approaching cloud system. Surface pressure charts showed a low

456 pressure system over Scandinavia (central pressure 1002 mb), with a warm front south east of
457 Svalbard that was moving north west. Surface winds in this area were $\sim 13 \text{ m s}^{-1}$ from the
458 north east. In-situ cloud microphysics measurements were made for approximately 1.5 hours
459 in total. To meet the objectives of the flight straight and level runs and saw tooth profiles
460 were performed through the cloud layers. Microphysics time series data from the flight are
461 shown in figure 8. Profile D2 is described below, with additional profile D1 discussed in
462 Appendix D The supplementary material. This second summer case was again found to have
463 different microphysical characteristics when compared with spring cases. Higher ice number
464 concentrations and the domination of the ice phase by secondary ice formation caused much
465 greater variability in the structure of the clouds observed.

467 **6.1 Profile D2**

468 During period ~~D1~~D2, the aircraft ~~also~~ performed a number of straight and level runs
469 combined with sawtooth profiles to capture the microphysical structure of the cloud layers
470 present. At 3100 m the aircraft flew a straight and level run below cloud base and
471 encountered a region of snow precipitation at temperatures between $-2 \text{ }^{\circ}\text{C}$ and $-3 \text{ }^{\circ}\text{C}$. N_{ice}
472 peaked at 5 L^{-1} giving peaks in calculated IWCs of $\sim 0.1 \text{ g m}^{-3}$. Probe imagery showed ice
473 crystals (mean diameter $410 \text{ }\mu\text{m}$) dominated by irregular particles, with some evidence of
474 plate like and dendritic structures. Observation of snow precipitation below some cloud
475 layers is a common observation in both spring and summer cases

476 During a ~~subsequent~~ profiled ascent up to 3400 m (to begin an extended SLR) the aircraft
477 penetrated cloud base at 3300 m ($T = -4 \text{ }^{\circ}\text{C}$). ~~By the top of the ascent~~ LWCs rose to $\sim 0.1 \text{ g}$
478 m^{-3} with N_{drop} generally observed to be between 10 and 50 cm^{-3} (mean diameter $12 \text{ }\mu\text{m}$). N_{ice}
479 in this region was between 0 and 1 L^{-1} ~~with peaks to 3 L^{-1}~~ and particlescrystals consisted of

480 irregular ice particles, columnar ice and small liquid droplets. The mean diameter of the ice
481 particles in this region was 470 μm . Continuing at 3400 m altitude, the aircraft encountered a
482 break in the cloud layer that lasted for around 1 minute (~ 6 km), before a subsequent cloud
483 layer was observed that had similar LWCs to the previous cloud layer ($\sim 0.1 \text{ g m}^{-3}$) but with
484 generally lower droplet concentrations (of mean diameter 17.5 μm); with mean N_{drop} values
485 of 15-30 cm^{-3} . N_{ice} values in this region were lower than before ($< 0.5 \text{ L}^{-1}$). The sampling of
486 this cloudy region was brief before another gap in cloud was observed that lasted ~ 2
487 minutes. The end of this second clear region was defined by a sudden transition to columnar
488 ice and small irregular particles (mean diameter 410 μm) in concentrations up to a peak of 4
489 L^{-1} . This region was mostly glaciated with $\text{LWC} < 0.01 \text{ g m}^{-3}$. During this SLR there were
490 very swift transitions observed between predominantly glaciated regions containing ice
491 crystals (peaking at 4 L^{-1}), of a columnar nature, and then mainly liquid regions consisting of
492 low concentrations ($< 30 \text{ cm}^{-3}$) of small liquid droplets (mean diameter 14 μm) and LWCs (\sim
493 0.01 g m^{-3}) (Fig 9c-d). This predominantly glaciated period ended when the aircraft
494 performed a profiled ascent and N_{ice} decreased to $< 0.5 \text{ L}^{-1}$ while LWCs increased to a peak of
495 0.3 g m^{-3} and N_{drop} rose to a maximum of $\sim 120 \text{ cm}^{-3}$ (mean diameter 14 μm). The aircraft
496 penetrated cloud top at 3,700 m ($T = -4.5 \text{ }^\circ\text{C}$). During subsequent passes through the H-M
497 zone during period D2 further peaks in ice concentrations upto 20 L^{-1} , attributed to rime-
498 splintering, were observed.

Formatted: Font: Italic, Subscript

499
500 ~~After climbing above cloud top, the aircraft performed a profiled descent back into the cloud~~
501 ~~layer to begin another SLR at 3400 m ($T = -4.5 \text{ }^\circ\text{C}$). At cloud top LWCs were $\sim 0.2 \text{ g m}^{-3}$~~
502 ~~N_{drop} peaked at 115 cm^{-3} . N_{ice} values were greater than in the previous cloud top region. There~~
503 ~~were two peaks of up to 15 L^{-1} with particle mean particle diameters of $\sim 370 \mu\text{m}$. Images~~
504 ~~show columnar particles, some of which had aggregated, were present together with small~~

505 liquid droplets (CDP mean diameter 11.5 μm). The second peak contained columnar ice
506 crystals of a similar size (mean diameter 400 μm). The largest spike in ice concentrations
507 occurred in close proximity to the first peak, with values as high as 20 L^{-1} observed, while
508 IWCs peaked at 0.15 g m^{-3} . Images showed irregular and columnar ice particles (mean
509 diameter 260 μm) present together with small liquid droplets (CDP mean diameter 12 μm)
510 (fig 9b). After these highs in ice number, concentrations declined to $\sim 2.5\text{ L}^{-1}$ before the
511 aircraft made a short profiled ascent and concentrations rose again to peak values of 10 L^{-1} .
512 At 3550 m cloud dissipated and the aircraft descended through a predominantly clear region
513 before reaching another significant cloud layer at 3450 m ($T = -4\text{ }^\circ\text{C}$). CDP N_{drop} and LWCs
514 were variable in this region with 10 second mean values rising to 145 cm^{-3} and 0.1 g m^{-3}
515 respectively. The droplets were small (mean diameter 8 μm) and ice was almost completely
516 absent during this part of the profile. After an SLR at 3,400m, the aircraft descended as the
517 cloud layer dissipated but encountered another, more significant layer around 3250 m ($T =$
518 $2.5\text{ }^\circ\text{C}$). LWCs increased to peak values of 0.4 g m^{-3} and droplet concentrations (mean
519 diameter 10.5 μm) increased to a peak of 410 cm^{-3} . This cloud layer was again predominantly
520 liquid. A spike in 2D-S concentrations was observed which imagery revealed was again due
521 to drizzle droplets. These data were removed from the ice dataset.

522

523 7.0 Primary IN Parameterization Comparison

Formatted: Font: Not Bold

524 Ice number concentrations as a function of altitude for science flight periods have been
525 presented and here these observations are compared to calculations of the primary IN
526 concentrations predicted using the D10 scheme, using aerosol concentrations (diameter > 0.5
527 μm) that were measured on each flight as input. DeMott et al. (2010) analysed datasets of IN
528 concentrations over a 14-year period from a number of different locations and found that

529 these could be related to temperature and the number of aerosol $> 0.5 \mu\text{m}$. The
530 parameterisation provided an improved fit to the datasets and predicted 62% of the
531 observations to within a factor of 2. Table 2 shows mean aerosol concentrations for
532 measurement periods during each case, the input temperature to *D10*, the maximum median
533 ice concentration used for comparison and the predicted IN concentration based on both the
534 PCASP and CAS aerosol measurements (where available). During the spring measurement
535 campaign it was possible to compare the CAS and PCASP probe data sets. Despite some
536 variation in concentrations reported between the two instruments, *D10* predicted IN values
537 were found to be fairly insensitive to these differences. Grosvenor et al. (2012) highlighted
538 that changes of about a factor of 4 produced a very limited change in the IN concentrations
539 predicted by the scheme.

540
541 In spring case 1 the maximum median ice value reached 0.61 L^{-1} so predicted IN values were
542 generally higher (between a factor of 2 and 4) than this median ice concentration observation.
543 However peaks in ice concentrations of up to $\sim 10 \text{ L}^{-1}$, were also observed (Fig. 2) so on
544 these occasions *D10* significantly under predicts observed ice number concentrations when
545 compared to these peak values. During spring case 2, maximum median ice concentration
546 values were similar to spring case 1. Secondary ice production was observed close to the sea
547 surface in this case so these higher median concentrations have been disregarded for the
548 purposes of the *D10* primary IN comparison. Aerosol measurements from the CAS were
549 lower than from the PCASP but predicted IN values were in good agreement (less than a
550 factor of 2) with the observed maximum median concentration. The peak concentrations
551 observed during the flight were $\sim 5 \text{ L}^{-1}$ (fig. 4) and as in the first spring case *D10* under
552 predicted these peak concentrations by about a factor of 10.

553
554 During summer case 1 the minimum cloud temperatures were higher ($T = -10\text{ }^{\circ}\text{C}$) than in the
555 spring cases. Maximum median ice concentrations observed were also higher (3.35 L^{-1}). The
556 origin of these enhanced concentrations is attributed to SIP, making a direct comparison with
557 the *D10* primary IN scheme difficult. Predicted IN concentrations from *D10* were found to
558 underestimate the maximum median ice concentrations observed in this summer case (due to
559 secondary ice production), but were in agreement with the concentrations observed near
560 cloud top, where the ice phase is likely to represent primary heterogeneous ice nucleation.
561 Observed ice concentrations in summer case 2 were also higher than in the previous spring
562 cases and similar to the first summer case. The second case had higher minimum cloud
563 temperatures than in the first summer case ($T = -4.3\text{ }^{\circ}\text{C}$). Due to effect of SIP at this
564 temperature, it was not possible to compare *D10* with the concentrations of ice observed in
565 these clouds.

Formatted: English (U.K.)

566
567 **8.0 Discussion**

Formatted: Font: Not Bold

568 Summaries of typical profiles during each case have been presented, with microphysics data
569 encompassing all cloud penetrations during the science flights presented as a function of
570 altitude shown in figures 10, 11 and 12. Figure 10 shows the cloud liquid droplet parameters,
571 figure 11 the ice crystal concentration statistics and figure 12 the ice mass and diameter
572 parameters. In each case (a) is spring case 1, (b) spring case 2, (c) summer case 1 and (d)
573 summer case 2. The yellow lines on the ice plots (Fig. 8) show the approximate location of
574 cloud top and cloud base altitudes deduced from liquid water content measurements
575 exceeding 0.01 g m^{-3} from the CDP. It is notable that droplet concentrations (Fig. 10) are
576 much higher in the second spring case than in the first spring case (max median values ~ 60

577 and $\sim 400 \text{ cm}^{-3}$ for spring case 1 and 2 respectively) and this is attributed to differences in
578 aerosol concentrations. N_{drop} are similar in the two summer cases (max median values 100 -
579 150 cm^{-3}) and lie between the two spring cases. The different aerosol loadings in spring case
580 1 and 2 may have led to the riming indirect effect playing a role in controlling the ice phase.
581 Case 2 had higher aerosol loadings and increased CCN availability, with smaller droplet sizes
582 (Fig. 10). In this case IWC values were also much lower than in the Case 1 and it is possible
583 that reduced riming efficiency of the smaller droplets contributed to reduced ice mass growth
584 through riming.

585
586 During the spring cases the mixed phase cloud layers were found to be approximately
587 adiabatic and exhibited generally uniform increases in LWC and droplet diameter (Fig. 10) to
588 liquid cloud tops that were observed to precipitate ice. At and above cloud top, well-defined
589 temperature inversions were present and dew points revealed a marked dry layer just above
590 cloud top. It was observed that cloud penetrated into the inversion layer, rather than being
591 capped below it. On average the cloud top was seen to extend $\sim 30 \text{ m}$ into the inversion layer
592 over which range the mean temperature increase was $\sim 1.6^\circ\text{C}$.

Formatted: English (U.S.)

593 -The ice phase is very likely to have been initiated through primary heterogeneous ice
594 nucleation in the temperature range spanned by these clouds (approximately $-10^\circ\text{C} > T > -20$
595 $^\circ\text{C}$). Generally low concentrations of ice crystals were observed (max median value 0.61 L^{-1})
596 (Table. 2), but with peaks up to $\sim 5\text{-}10 \text{ L}^{-1}$ in both spring cases (Fig. 11). Cloud top regions
597 consisted of small liquid droplets (median diameter ~ 15 and $25 \mu\text{m}$ for spring cases 1 and 2
598 respectively) (Fig. 10a-b), together with small irregular ice crystals (Fig 3a and Fig 5a). In
599 both of these cases, ice crystal diameter increased to maximum values of $530 \mu\text{m}$ and $660 \mu\text{m}$
600 respectively (Fig. 12a-b). The variability in ice crystal diameter (fig. 12a-b) shows periods

601 where maximum ice crystal diameters increased to ~ 2 mm. These crystals were often
602 comprised of a mixture of large rimed irregular particles (Fig. 3 and 5) and dendritic snow
603 crystals. Median IWC values in the spring cases reached ~ 0.01 g m⁻³ (Fig. 12a-b), with peak
604 values during case 1 up to ~ 0.3 g m⁻³ compared with 0.1 g m⁻³ in case 2. The highest Median
605 LWCs (Fig. 10) were observed at cloud top during spring cases, peaking at 0.3 and 0.5 g m⁻³
606 during cases 1 and 2 respectively. While these clouds were seen to be fairly uniform, time
607 series data (Fig. 2 and 4) show some of the variability in the microphysics that was observed
608 during the science flight.

609 |
610 During the summer cases, the cloud layers spanned a higher temperature range (-10 °C < T <
611 0 °C) and well-defined temperature inversions at cloud top were less evident. There was a
612 much greater tendency towards there being multiple cloud layers that were shallower and less
613 well coupled. During summer case 2 a significant temperature inversion was observed (Fig.
614 10d) in the cloud base region, which suggested a de-coupling of the boundary layer and the
615 cloud system above. Liquid cloud top regions with few (generally < 1 L⁻¹) ice crystals,
616 formed through heterogeneous ice nucleation at these temperatures, were observed in both
617 cases (Fig. 11c-d). LWCs in summer case 1 were lower than the spring cases (median values
618 $< \sim 0.1$ g m⁻³) and similar in shape to the uniform profiles seen in the spring cases. The
619 second summer case had higher median LWCs (up to 0.35 g m⁻³) and showed much more
620 variability with a number of increases and decreases in median LWC values with altitude
621 (Fig. 10d).

622 Median cloud top ice concentrations in summer case 1 were similar to the spring cases (~ 0.2
623 L⁻¹) (fig. 11d), however maximum median values lower down in the cloud reached 3.35 L⁻¹
624 (Table 2), about a factor of 14 higher than in the spring cases. Peaks in ice number

625 concentrations around the $-5\text{ }^{\circ}\text{C}$ level reached between $30\text{--}40\text{ L}^{-1}$. During the summer, the
626 clouds spanned the temperature range -3 to -8°C , where a well-known mechanism of
627 secondary ice production operates through splintering during riming; the Hallet-Mossopp
628 process (H-M). The observations in this case, of liquid water together with ice particles at
629 temperatures around $-5\text{ }^{\circ}\text{C}$, are consistent with this process being active and enhancing ice
630 number concentrations (Fig 7 and 9). Time series (Fig. 6 and 8) showed more variation than
631 in the spring cases. Distinct liquid cloud tops were still evident, but at lower altitudes
632 significant variations in LWCs, droplet number concentrations and ice number concentrations
633 were seen together with gap regions where little or no cloud was present. On a number of
634 occasions predominantly liquid conditions were swiftly replaced by regions of high
635 concentrations of columnar ice crystals. Some of these transitions took place over ~ 1 second
636 or horizontal distance of the order 60 m . These rapid fluctuations were attributed to the
637 contributions from the H-M process. The process of glaciation through secondary
638 enhancement of ice number concentrations is likely to have caused some of this increased
639 variability in cloud properties too, with liquid droplets quickly being removed through
640 depletion of liquid water by the ice phase. The cloud layers during summer case 2 spanned a
641 higher temperature range than summer case 1. Cloud tops were around $-4\text{ }^{\circ}\text{C}$, and median ice
642 number concentrations reached maximum values of 2.5 L^{-1} , about an order of magnitude
643 higher than in the spring cases. Time series (Fig. 8) and percentile plots (Fig. 11d) showed
644 peaks in ice number concentrations to $\sim 25\text{ L}^{-1}$ and in these regions probe imagery revealed
645 distinctive columnar ice crystals likely to have grown from splinters produced via H-M, into
646 habits typical of growth at these temperatures around $-4\text{ }^{\circ}\text{C}$. In addition, the formation of
647 high ice concentrations may have led to the dissipation of some liquid cloud regions below
648 cloud top due to consumption of the liquid phase by ice crystals growing by vapour diffusion
649 (i.e. ice crystal growth via the Bergeron-Findeisen (B-F) process (Bergeron, 1935). This is

650 consistent with the observed summer clouds being more broken than the clouds observed
651 during spring. However, as discussed in the introduction, it is also recognised that cloud-
652 radiation interactions may lead to the separation of cloud layers during the Arctic summer.

653
654 Comparison of the observed N_{ice} with the *D10* parameterization of primary ice nuclei
655 numbers revealed that during the spring case 1, maximum median N_{ice} was lower than the
656 primary IN concentrations predicted by *D10*, but similar in spring case 2. Peaks in N_{ice} were
657 much higher than the *D10* IN predictions, by an amount depending on the aerosol
658 measurement period used as input to *D10* (Table 2). Our observations show deviation in the
659 ice concentrations as high as an order of magnitude compared with the *D10* IN prediction.
660 The variation in ice number concentrations observed in the spring cases could be explained
661 by the variability in observed IN values presented in the DeMott et al. (2010) paper.

662 In the summer cases the enhancement of N_{ice} through the H-M process made a realistic
663 comparison difficult. Despite this difficulty, the first summer case had cloud top temperatures
664 that were just outside the H-M temperature zone ($-10\text{ }^{\circ}\text{C}$) and median N_{ice} in this region was \sim
665 0.2 L^{-1} , which is within a factor of 2 of values predicted by *D10* (Table 2). At lower altitudes
666 the increase in cloud temperatures allowed rime-splintering to enhance concentrations to
667 above what would be expected via primary heterogeneous ice nucleation. In the second
668 summer case cloud top temperatures were higher ($-4\text{ }^{\circ}\text{C}$), and enhancement of the ice crystal
669 number concentrations through SIP prevented observations of any first ice by primary
670 nucleation being made. Ice crystal number concentrations were thus enhanced to values
671 above what was predicted by *D10* throughout the depth of the cloud. ~~Whilst primary ice~~
672 ~~nucleation is identified as the most important ice forming process in the spring clouds, the~~
673 ~~summer stratocumulus ice concentrations were dominated by secondary ice production via~~

674 ~~the H-M process as discussed. Due to this SIP enhancement, ice concentrations in summer~~
675 ~~reached much higher values than those observed anywhere in the spring cases.~~

676

677 The microphysical structure of the spring and summer stratocumulus layers was found to be
678 consistent with previous observations of arctic clouds. We observed generally low droplet
679 number concentrations ~~with increased concentrations~~that were enhanced during incursions of
680 higher aerosol loadings. ~~This is consistent with observations, similar to findings~~ by Verlinde
681 et al. (2007). During spring cases, LWCs and liquid droplet size increased uniformly to cloud
682 top, however during summer months the vertical structure of cloud layers was more variable
683 (e.g. Hobbs and Rangno, 1998). During spring cases in particular, liquid cloud tops at distinct
684 temperature inversions continually precipitated low concentrations of ice into the cloud
685 below, which has been observed previously in the Arctic. ~~Rogers et al. (2001) made airborne~~
686 ~~measurements of IN in thin, low-level arctic clouds in the same temperature range as our~~
687 ~~spring cases. They found evidence for a few IN in these clouds with concentrations of ice that~~
688 ~~were similar to the observations presented here.~~

689 During the Arctic summer, Hobbs and Rangno (1998) observed generally higher ice
690 concentrations with columnar and needle ice crystals in concentrations of 'tens per litre'
691 where stratocumulus cloud top temperatures were between -4°C and -9°C. ~~Rangno and~~
692 ~~Hobbs (2001) found that high ice particle concentrations were common during late spring and~~
693 ~~summer in the Arctic. Despite the presence of some columnar ice, many of the crystals were~~
694 ~~irregular in shape, and it was suggested that shattering of freezing drops > 50 µm or the~~
695 ~~fragmentation of fragile ice may have contributed to the high concentrations. Although we~~
696 ~~have not performed habit classification analysis on our dataset the images suggest that the ice~~
697 ~~phase in summer cases was dominated by columnar ice, with evidence of a small number of~~

698 irregular ice particles. Previous laboratory studies found that larger droplets were necessary
699 to initiate rime-splintering (Mossop, 1985) and Hobbs and Rangno confirm that in the cases
700 they studied a threshold droplet size of 28 μm was required, below which secondary ice
701 production did not take place. In the limited summer cases we had in the appropriate
702 temperature range secondary ice production took place in the presence of concentrations of
703 liquid droplets over this threshold size.

704 The summer cases we observed contained median values of N_{ice} that were 4-6 times greater
705 than we observed in the spring cases. ~~In the spring, the cloud layers were colder than the~~
706 ~~temperature range within which H-M is active, and accordingly contained peak~~
707 ~~concentrations of ice closer to predictions from D10. In the summer cases, the clouds spanned~~
708 ~~a warmer temperature range between about 0 °C and -10 °C, leading to low concentrations of~~
709 ~~primary ice that when conditions became suitable, were then enhanced through rime-~~
710 ~~splintering. During the spring we also observed cloud that~~ In both summer cases where the H-
711 M process was active droplet sizes were similar, and we didn't find any evidence for a
712 thermodynamic indirect effect leading to differences in the efficiency of secondary ice
713 production in summer cases. ~~penetrated into the inversion layer, rather than being capped~~
714 ~~below it. On average the cloud top was seen to extend ~30 m into the inversion layer over~~
715 ~~which range the mean temperature increase was ~1.6 °C.~~

Formatted: English (U.S.)

716
717 Changes in aerosol concentrations and composition have been suggested as a possible factor
718 in explaining previous observations of the glaciation of arctic clouds at different temperatures
719 (Curry et al., 1996). During spring case 2 higher concentrations of aerosol were observed
720 when compared to spring case 1. Droplet number concentrations were also much higher in
721 spring case 2, generally 300-400 cm^{-3} in comparison to spring case 1 where concentrations

722 were generally $\sim 50\text{-}100\text{ cm}^{-3}$. Despite this, no significant difference was observed in the ice
723 number concentrations. However, it should be noted that despite the higher total
724 concentrations, the population of aerosol $> 0.5\text{ }\mu\text{m}$ was not significantly enriched in spring
725 case 2 compared to the spring case 1. *D10* has a dependency only on this portion of the
726 aerosol size distribution, so may explain the similar primary ice number concentrations for
727 both spring case studies. Although we didn't make any direct measurements of IN, in both
728 Arctic spring cases and Antarctic cases primary heterogeneous ice nucleation was identified
729 as the dominant source of ice. It's very likely that the higher concentrations of ice in the
730 Arctic cases when compared to the Antarctic were therefore due to increasing IN availability,
731 which is consistent with the glaciation indirect effect.

732
733 Grosvenor et al. (2012) studied stratocumulus clouds in the Antarctic over the Larsen C ice
734 shelf. These observations contained periods where temperatures were comparable to those in
735 the spring cases studied here. The lower layers of Antarctic cloud were also reported to
736 contain higher concentrations of ice produced via the H-M process, similar to the summer
737 cases that we have discussed. A summary of some of the measurements reported from the
738 Antarctic in Grosvenor et al. (2012) can be found in Table 3. Measurements of cloud regions
739 outside the H-M temperature zone revealed very low ice number concentrations, with
740 maximum values about 2 orders of magnitude lower than those observed in the spring cases
741 reported here. Aerosol concentrations from a CAS probe (similar to the one deployed in this
742 study) reported generally lower concentrations of aerosol particles $D_p > 0.5\text{ }\mu\text{m}$. The *D10* IN
743 predictions in the Antarctic were reported to compare better with maximum, rather than mean
744 ice values. A similar result was found in this study where predicted primary IN values were
745 greater than observed median values. However, when comparing with peak ice concentration
746 values the scheme significantly under-predicted these. Grosvenor et al. (2012) discussed the

747 possibility that due to the *D10* parameterisation being based on mean IN concentrations from
748 many samples, the finding that IN predictions compared well with the maximum values
749 rather than mean values may suggest the scheme was over predicting IN concentrations
750 generally in the Antarctic (for these particular cases at least). In the H-M layer in the
751 Antarctic over Larsen C, ice crystal number concentrations were found to be higher than
752 those observed in colder temperature regimes (not spanning the H-M temperature range), in
753 keeping with the findings from the Arctic presented this paper. However the concentrations
754 produced by the H-M process in the Antarctic were generally only a few per litre,
755 approximately an order of magnitude lower than those observed during the summer cases in
756 the Arctic.

Formatted: English (U.S.)

758 9.0 Conclusions

759 Detailed microphysics measurements made in Arctic stratocumulus cloud layers during the
760 early spring and summer, have been presented.

761

762 • Two spring and two summer cases were presented. The cloud layers during summer
763 cases spanned a warmer temperature range ($\sim 0\text{ }^{\circ}\text{C} \geq T > -10\text{ }^{\circ}\text{C}$) than in spring
764 (generally $\sim -10\text{ }^{\circ}\text{C} \geq T > -20\text{ }^{\circ}\text{C}$).

765

766 • Spring case 2 had significantly higher aerosol concentrations ($\sim 300\text{-}400\text{ cm}^{-3}$)
767 compared to the first spring case ($\sim 50\text{-}100\text{ cm}^{-3}$). Despite this difference, ice number
768 concentrations were found to be similar in both spring cases, suggesting the source of

769 the increased aerosol concentrations was not providing additional IN that were
770 efficient over the temperature range $-10\text{ }^{\circ}\text{C} > T > -20\text{ }^{\circ}\text{C}$.

771 |
772 • In the spring cases, cloud layers appeared more uniform with steady increases in
773 LWC and cloud droplet size to cloud top, where low concentrations ($< 1\text{ L}^{-1}$) of ice
774 were frequently observed to precipitate through the depth of the cloud layer. The
775 small irregular particles observed at cloud top grew to a median diameter $\sim 500\text{ }\mu\text{m}$ in
776 both cases with peaks in diameter $> 1000\text{ }\mu\text{m}$ as the crystals descended through the
777 cloud. 2D-S imagery revealed the dominant growth habit to be dendritic in nature.
778 The summer cases consisted of multiple cloud layers that were observed to be more
779 variable than in the spring. However, liquid cloud top regions were still evident and
780 ice was again observed to precipitate into the cloud layers below.

781 |
782 • The maximum median ice number concentrations observed within cloud layers during
783 the summer cases were approximately a factor of 5 (or more) higher than in the spring
784 cases. This enhancement in the ice number concentrations is attributed to the
785 contribution of secondary ice production through the H-M process.

786 • This finding suggests that low level summer stratocumulus clouds situated in the H-M
787 temperature zone in the Arctic may contain significantly higher ice number
788 concentrations than in spring clouds due to the temperature range of the former
789 spanning the active H-M temperature zone.

790 |

791 • Predicted values from the DeMott et al. (2010) scheme of primary ice nuclei, using
792 aerosol measurements obtained during the science flights as input, tended to
793 overpredict IN concentrations compared to the observed maximum median ice crystal
794 number concentrations during the spring, but under-predict IN when compared to
795 peak ice crystal concentrations. This variation can be attributed to uncertainties in the
796 application of the DeMott scheme. During the summer cases, due to contributions
797 from secondary ice production, the scheme predicted significantly lower values of ice
798 particles than those observed.

799
800 • We found some support for the riming indirect effect when comparing our spring
801 cases. In spring case 2 higher aerosol loadings and smaller droplets were observed and
802 ice water contents were lower than in spring case 1 (where aerosol concentrations
803 were much lower). It is possible the smaller droplets in case 2 reduced the riming
804 efficiency leading to lower ice mass values.

805 • Grosvenor et al. (2012) observed lower concentrations of aerosol $> 0.5 \mu\text{m}$ in the
806 Antarctic when compared to similar measurements made in the Arctic. They found
807 that IN predictions using *D10* agreed better with their observed peak ice concentration
808 values rather than their maximum mean values. They measured approximately an
809 order of magnitude lower primary ice concentrations in summer Antarctic clouds than
810 in our spring Arctic cases, but did observe enhancement through SIP in warmer cloud
811 layers where concentrations increased to a few per litre. These were still about an
812 order of magnitude less than the enhanced concentrations observed in the Arctic
813 summer cases presented here, but were similar to the peak values observed in spring
814 cases over the Arctic (where no SIP was observed).

815

816 **Appendix A**

817 **Profiled Ascent A1**

818 During profile A1 the aircraft (travelling south) made a profiled ascent from 300 m above the
819 sea surface, reaching cloud base at 650 m, identified using a Liquid Water Content threshold
820 of $LWC > 0.01 \text{ g m}^{-3}$, as derived from CDP data. Below cloud base the 2D-S probe revealed
821 low concentrations ($< 0.5 \text{ L}^{-1}$) of irregular snow (Fig. 3d) particles (mean size $\sim 530 \text{ }\mu\text{m}$) that
822 had precipitated from the cloud layer above. As the aircraft climbed through cloud base,
823 temperatures decreased to $-11 \text{ }^\circ\text{C}$. CDP droplet concentrations (N_{drop}) (10 second averaged
824 values) increased to $\sim 80 \text{ cm}^{-3}$, LWCs peaked at $\sim 0.2 \text{ g m}^{-3}$ and mean droplet diameters were
825 $\sim 8 \text{ }\mu\text{m}$. Measurements from the 2D-S showed ice crystals with mean size $\sim 415 \text{ }\mu\text{m}$ in low
826 concentrations, $\sim 1 \text{ L}^{-1}$. Images from the 2D-S revealed irregular snow particles with some
827 dendritic habits coexisting with small liquid droplets. As the ascent continued the aircraft
828 encountered a layer containing higher N_{ice} at $-14 \text{ }^\circ\text{C}$. Ice crystals consisted of snow particles
829 (mean size $350 \text{ }\mu\text{m}$) in concentrations $\sim 4 \text{ L}^{-1}$. Probe imagery showed these to be a mixture of
830 large irregular ice crystals, small, more pristine plate-like crystals and some crystals with
831 columnar habits. The highest 10 second mean N_{ice} reached $\sim 6 \text{ L}^{-1}$ with peak values $\sim 15 \text{ L}^{-1}$.
832 These were observed in a region approximately 500 m below cloud top. Maximum 10 second
833 averaged Ice Water Content (IWC) reached 0.2 g m^{-3} with peaks up to 0.3 g m^{-3} in the same
834 region. Particle images here revealed (Fig 3b) irregular ice crystals together with a few
835 smaller pristine plates. The mid-region of this stratocumulus deck also consisted of liquid
836 droplets (mean diameter $\sim 13 \text{ }\mu\text{m}$) in concentrations $\sim 75 \text{ cm}^{-3}$, and LWC $\sim 0.3 \text{ g m}^{-3}$, with
837 some 1 second integration periods being as high as 0.5 g m^{-3} . As the aircraft approached
838 cloud top, where the lowest temperature recorded was $-19.5 \text{ }^\circ\text{C}$, N_{ice} reduced to $\sim 0.5 \text{ L}^{-1}$ with

839 mean sizes of 285 μm , however this region was dominated by liquid droplets (mean diameter
840 17 μm) with N_{drop} up to 95 cm^{-3} , and LWC values peaking at 0.7 g m^{-3} . Imagery from the 2D-
841 S revealed many small droplets together with numerous small irregular ice crystals in this
842 cloud top region. After measuring the vertical structure of the cloud layer, which was
843 approximately 1 km in depth, the aircraft penetrated cloud top at 1675 m and passed through
844 an inversion layer where the temperature increased to $-13\text{ }^{\circ}\text{C}$.

845 **Profiled Descent A3**

846 Following another ascent, the aircraft performed a profiled descent (A3) from the inversion
847 layer, $T=-13\text{ }^{\circ}\text{C}$, penetrating cloud top at 1,569 m asl where $T=-16\text{ }^{\circ}\text{C}$. As the aircraft
848 descended, LWC increased rapidly to 0.9 g m^{-3} at 30 m below cloud top, the highest LWC
849 recorded at any point during the flight. Mean droplet diameters in this region were $\sim 23\text{ }\mu\text{m}$ in
850 concentrations of $\sim 90\text{ cm}^{-3}$. 2D-S images revealed many small liquid droplets with a few
851 small (mean diameter 190 μm) irregular ice crystals (Fig. 3a) with $N_{ice}\sim 1\text{ L}^{-1}$. The region
852 immediately below this cloud top layer, between 1520 and 1275 m, exhibited a steady decline
853 in LWC while droplet concentrations and N_{ice} maintained similar values to those observed in
854 the cloud top region. Mean ice crystal diameters increased markedly to 520 μm before LWCs
855 eventually fell to below the threshold value (0.01 g m^{-3}), marking the base of an upper layer
856 of cloud. A subsequent cloud layer, 750 m below, was then encountered. In the clear air
857 region separating these two cloud layers temperatures rose by around $5\text{ }^{\circ}\text{C}$ to $-11\text{ }^{\circ}\text{C}$ and
858 large ($\sim 760\text{ }\mu\text{m}$) irregular snow particles, some of which exhibited dendritic growth habits,
859 were observed. Precipitation concentrations were generally $< 0.5\text{ L}^{-1}$. Mean IWCs in this
860 precipitation zone were $\sim 0.01\text{ g m}^{-3}$. The particles observed falling from the higher cloud
861 layer descended into the cloud layer below at 1,275m asl. In the top of this lower cloud layer
862 ($T=-11\text{ }^{\circ}\text{C}$) LWCs rose to 0.4 g m^{-3} with N_{drop} (mean diameter 15 μm) increasing to $\sim 120\text{ cm}^{-3}$
863 while N_{ice} increased to $\sim 1\text{ L}^{-1}$, 2D-S probe imagery in this region revealed the presence of

864 larger snow particles (mean diameters $\sim 815 \mu\text{m}$). As the aircraft descended further, LWCs
865 gradually decreased while N_{drop} remained fairly constant before reaching cloud base at 280 m,
866 (much closer to sea level than in profiles A1 and A2). Below cloud base precipitating snow
867 (mean particle size $\sim 625 \mu\text{m}$) was observed.

868 **Appendix B**

869 **Profiled Ascent B2**

870 During profiled Ascent B2 (prior to profile descent B1 above) the aircraft climbed from
871 below cloud base at 190 m ($T = 5^\circ\text{C}$) travelling initially through snow precipitation in
872 concentrations peaking at $\sim 3 \text{L}^{-1}$ (mean diameter $420 \mu\text{m}$). Images revealed dendritic ice
873 crystals that had descended from the cloud layer above (fig. 5c). IWCs in this region peaked
874 at 0.025g m^{-3} . Cloud base during this profile was less well defined than in later ascents with
875 variable LWCs and droplet number concentrations before a more defined cloud base was
876 encountered at 1010 m. N_{drop} then increased rapidly to 270cm^{-3} (mean diameter $\sim 12.5 \mu\text{m}$)
877 while LWCs increased more gradually to $\sim 0.4 \text{g m}^{-3}$. N_{ice} through this region showed a
878 decline to $< 0.1 \text{L}^{-1}$, and consisted of precipitating snow particles with a mean diameter of
879 $430 \mu\text{m}$. Closer to cloud top (1410 m) ice crystal number concentrations increased, to peak
880 values of $\sim 1 \text{L}^{-1}$. Images (fig. 5b) showed smaller crystals (mean diameter $\sim 370 \mu\text{m}$) at this
881 higher altitude, with evidence of hexagonal habits and peak values of IWC $\sim 0.04 \text{g m}^{-3}$.
882 Droplet concentrations towards cloud top were similar to lower in the cloud, while LWCs
883 increased to 0.6g m^{-3} and mean droplet diameter increased to $\sim 15 \mu\text{m}$. The coldest
884 temperature reached within the cloud layer was -18°C , but cloud top (at $\sim 1530 \text{m}$) was
885 warmer by 1°C . A further increase of 1°C was observed as the aircraft ascended through the
886 inversion layer. The depth of this cloud layer (520 m) was significantly less than that
887 observed during the previous spring case cloud layer penetrations.

888 **Constant Altitude Runs B3 and B4**

889 During straight and level run (SLR) B3 the aircraft flew below cloud base at 390 m asl to
890 characterise precipitation. During B3 the aircraft briefly traversed a region of low cloud with
891 high N_{drop} (peaking at $\sim 520 \text{ cm}^{-3}$) but generally low LWCs ($< 0.1 \text{ g m}^{-3}$). These cloud
892 droplets were small (mean diameter $\sim 6 \mu\text{m}$). 2D-S imagery also revealed small drops were
893 present together with snow crystals (mean diameter $\sim 370 \mu\text{m}$) that were precipitating into
894 these brief regions of low cloud. During B3 temperatures increased from $-12 \text{ }^\circ\text{C}$ to $-10 \text{ }^\circ\text{C}$.
895 Crystal habits in the out of cloud regions were dominated by aggregates of dendrites and
896 some pristine ice crystals ($\sim 0.5 \text{ L}^{-1}$). Here, LWCs were below 0.01 g m^{-3} , although the 2D-S
897 also detected drizzle droplets precipitating from the cloud layer above (mean concentration \sim
898 0.2 L^{-1}). Later in B3 the aircraft left its constant altitude and descended to 80 m asl ($T = -8.5$
899 $^\circ\text{C}$). Mean N_{ice} increased to $\sim 2 \text{ L}^{-1}$ with peaks up to 4 L^{-1} . There was a corresponding
900 increase in 2D-S droplet concentrations to a mean of $\sim 1 \text{ L}^{-1}$. 2D-S imagery shows the
901 presence of small columnar shaped ice crystals (similar to those shown in figure 5d), together
902 with larger snow particles and drizzle droplets. CDP LWC was $< 0.01 \text{ g m}^{-3}$ in this region,
903 since the larger drizzle droplets measured by the 2D-S were outside the CDP size range. In
904 this region of enhanced N_{ice} , just above the sea surface, IWCs, which were generally $< 0.01 \text{ g}$
905 m^{-3} in the below cloud base region, increased to peak values of 0.04 g m^{-3} .

906 At the start of run B4, prior to undertaking a mainly straight and level run (SLR) initially to
907 the NW, the aircraft first descended from the inversion layer ($T = -14 \text{ }^\circ\text{C}$) into the cloud top
908 (1050 m asl). LWC initially rose sharply to a peak of 0.5 g m^{-3} before gradually falling away
909 to a mean value $\sim 0.3 \text{ g m}^{-3}$. Mean droplet concentrations over a ~ 5 minute period were 340
910 cm^{-3} (mean diameter $11 \mu\text{m}$) and the 2D-S imagery revealed the presence of small droplets
911 together with large snow crystals (mean diameter $730 \mu\text{m}$) in concentrations $< 0.1 \text{ L}^{-1}$ and
912 IWCs of 0.03 g m^{-3} . At 1240 UTC a generally cloud free region was encountered and

913 sampled for ~4 minutes before re-entering cloud again. During this period the aircraft was
914 turned onto a reciprocal heading at the NW limit of its track. Cloud microphysics
915 measurements revealed this cloud top region to be very similar to the first period during B4.
916 Mean values of LWC over ~4 minute period were 0.2 g m^{-3} , droplet concentrations (mean
917 diameter $\sim 9 \text{ }\mu\text{m}$) were $\sim 340 \text{ cm}^{-3}$. N_{ice} while generally less than 1 L^{-1} (IWC $\sim 0.01 \text{ g m}^{-3}$)
918 showed brief increases (during 1 second integration periods) to 2 L^{-1} and IWC values peaked
919 at 0.1 g m^{-3} . 2D-S imagery showed the presence of dendritic ice particles (mean diameter 750
920 μm) together with small spherical particles, likely to be liquid droplets. Temperatures in the
921 cloud top regions remained fairly constant throughout B4 (between $-15 \text{ }^\circ\text{C}$ and $-16 \text{ }^\circ\text{C}$). The
922 aircraft flew above cloud top for the remainder of the SE-bound leg, and found there to be no
923 ice particles falling into cloud top from above.

924 **Appendix C**

925 **Stepped Run C1**

926 The BAS aircraft performed a stepped profile (flight segments C1.1–C1.4) from a cloud top
927 altitude of $\sim 3000 \text{ m}$ down to 2249 m covering the temperature range $-7.5 \text{ }^\circ\text{C}$ to $-2 \text{ }^\circ\text{C}$. In total
928 4 SLRs and 4 profiled descents were carried out during this run. During the first penetration
929 of cloud (run C1.1), N_{drop} over a 2 minute period was 240 cm^{-3} . LWCs rose to $\sim 0.1 \text{ g m}^{-3}$ and
930 the droplet mean diameter was $10.5 \text{ }\mu\text{m}$. N_{ice} was generally very low during this period < 0.25
931 L^{-1} with some peaks up to 0.5 L^{-1} . During C1.1 the aircraft maintained an altitude of $\sim 3000 \text{ m}$
932 for several minutes. The cloud microphysics remained predominantly stable, with low N_{ice} ($<$
933 0.25 L^{-1}) and LWCs $\sim 0.01 \text{ g m}^{-3}$. The only notable change was a slight increase in the mean
934 diameter of droplets measured by the CDP to $11.5 \text{ }\mu\text{m}$ and a reduction in number
935 concentration to 185 cm^{-3} . At $\sim 0900 \text{ UTC}$ the aircraft descended $\sim 100 \text{ m}$ to start run C1.2
936 ($T = -6 \text{ }^\circ\text{C}$), and encountered a cloud sector where N_{ice} increased to 2 L^{-1} with peaks to 5 L^{-1}

937 (and IWC peaks up to 0.03 g m^{-3} observed here). 2D-S imagery (Fig 7a) revealed irregular ice
938 crystals and the presence of columnar ice both of which appeared to be rimed. Many small
939 single-pixel ($10 \text{ }\mu\text{m}$) particles were also measured. These likely represent the small droplets
940 detected by the CDP in this region (mean diameter $13.5 \text{ }\mu\text{m}$) in concentrations of 125 cm^{-3} .
941 Later during C1.2, N_{ice} fell to values $< 0.25 \text{ L}^{-1}$. The aircraft performed a profiled descent at
942 the start of C1.3, descending 200 m to $\sim 2720 \text{ m}$ ($T = -4^\circ\text{C}$). During the descent, LWCs and
943 droplet number concentrations fell to near zero values while N_{ice} increased to peak values of 5
944 L^{-1} (and IWC peaked at 0.02 g m^{-3}). 2D-S images again revealed the presence of small (mean
945 diameter $255 \text{ }\mu\text{m}$) rimed irregular ice crystals and ice crystals of columnar habit. In the
946 temperature range spanned by this cloud, these observations are consistent with the
947 contribution of secondary ice production (SIP) through rime splintering. During C1.3 further
948 N_{ice} peaks up to 5 L^{-1} consisting of columnar particles and irregular ice crystals were observed
949 (fig 7b). The liquid phase of the cloud in this region was much more variable than nearer to
950 cloud top. Increases in peak LWCs to 0.01 g m^{-3} were seen together with an increase in
951 droplet number concentrations to $\sim 150 \text{ cm}^{-3}$ (mean diameter $13.5 \text{ }\mu\text{m}$). These occurred
952 between periods where LWC values were near zero and the cloud was predominantly
953 glaciated.

954

955 During C1.4 the aircraft descended 300 m to $2,450 \text{ m}$ ($T = -3^\circ\text{C}$). During this run the time
956 between peaks in N_{drop} increased, while the highest N_{ice} measured during this science flight
957 were observed (peaking at $N_{ice} = 35 \text{ L}^{-1}$). IWCs peaked at 0.2 g m^{-3} , which is significantly
958 greater than values observed elsewhere in this cloud system. 2D-S imagery (fig. 7c) reveals
959 that these high ice crystal number concentrations were dominated by columns (mean diameter
960 $260 \text{ }\mu\text{m}$), which at times were seen together with small liquid droplets. These observations
961 are consistent with SIP through the H-M process.

962 **Appendix D**

963 **Profiled descent D1**

964 Well into the flight, the BAS aircraft performed a profiled descent from cloud top at 3,700 m
965 to 2,400 m over the temperature range -5.2°C to 3°C . At cloud top, LWCs rose to a peak of
966 0.3 g m^{-3} , with peak N_{drop} (mean diameter $12.5\text{ }\mu\text{m}$) up to 270 cm^{-3} . N_{ice} , initially close to
967 zero, rose to peaks of 6 L^{-1} with IWCs up to 0.1 g m^{-3} . 2D-S images (fig. 9a) showed
968 columnar ice crystals (mean diameter $350\text{ }\mu\text{m}$) in this region, together with liquid droplets. At
969 times swift transitions between predominantly liquid and glaciated conditions were observed.
970 At 3,500 m ($T = -3.5^{\circ}\text{C}$) the CDP stopped measuring significant values of LWC ($> 0.01\text{ g m}^{-3}$)
971 and this appeared to mark a gap region in the cloud layer of approximately 100 m in depth.
972 The 2D-S did detect low N_{ice} in this region. These were generally below $< 0.5\text{ L}^{-1}$. When the
973 aircraft descended into the lower cloud layer ($T = -2^{\circ}\text{C}$) LWCs increased to peak values of 1
974 g m^{-3} , where N_{drop} (mean diameter $13.5\text{ }\mu\text{m}$) increased to values as high as 250 cm^{-3} . 2D-S
975 imagery revealed few ice crystals in this region but high drizzle drop concentrations.

976

977 At 2,800 m ($T = 0^{\circ}\text{C}$) a further period of drizzle droplets was observed in the 2D-S imagery.
978 These again appeared stretched and made it impossible to separately identify ice in the data
979 set, so there is no reliable ice crystal mass and number concentration data in this region. At
980 this time, CDP LWCs peaked at 0.4 g m^{-3} and droplet concentrations varied from close to
981 zero to up to $\sim 350\text{ cm}^{-3}$. The mean diameter of the droplets measured by the CDP was 10
982 μm . As the aircraft descended towards its minimum descent altitude large variations in LWCs
983 and droplet concentrations continued to be observed with peaks up to 0.2 g m^{-3} and 420 cm^{-3}
984 respectively.

985 Acknowledgements.

986 This project was supported by the Natural Environment Research Council under grant
987 NE/1028296/1. Airborne data was obtained using the BAe-146-301 Atmospheric Research
988 Aircraft [ARA] flown by Directflight Ltd and managed by the Facility for Airborne
989 Atmospheric Measurements (FAAM), which is a joint entity of the Natural Environment
990 Research Council (NERC) and the Met Office.

991

992 **References**

Formatted: Font: Not Bold

993 **Bibliography**

994

995 Baker, B. and Lawson, P.: Improvement in Determination of Ice Water Content from Two-
996 Dimensional Particle Imagery . Part I: Image-to-Mass Relationships, J. Appl. Meteorol.
997 Climatol., 45, 1282–1290, 2006.

998 Baumgardner, D., Jonsson, H., Dawson, W., O'Connor, D. and Newton, R.: The cloud,
999 aerosol and precipitation spectrometer: a new instrument for cloud investigations, *Atmos.*
1000 *Res.*, 59-60, 251–264, doi:10.1016/S0169-8095(01)00119-3, 2001.

1001 Bergeron, T.: On the physics of clouds and precipitation, *Proces Verbaux de l'Association de*
1002 *Météorologie, International Union of Geodesy and Geophysics*, 156–178, 1935.

1003 Brown, P. and Francis, P.: Improved measurements of the ice water content in cirrus using a
1004 total-water probe, *J. Atmos. Ocean. Tech.*, 12, 410–414, 1995.

1005 Callaghan, T. V., Johansson, M., Key, J., Prowse, T., Ananicheva, M. and Klepikov, A.:
1006 Feedbacks and Interactions: From the Arctic Cryosphere to the Climate System, *Ambio*, 40,
1007 75–86, doi:10.1007/s13280-011-0215-8, 2012.

1008 Crosier, J., Bower, K. N., Choullarton, T. W., Westbrook, C. D., Connolly, P. J., Cui, Z. Q.,
1009 ---Blyth, aA. M. (2011). Observations of ice multiplication in a weakly convective cell
1010 embedded in supercooled mid-level stratus. *Atmospheric Chemistry and Physics, Atmos.*
1011 *Chem. Phys.*, 11(1), 257–273. doi:10.5194/acp-11-257-2011

Formatted: Font: Not Italic

1012 Crosier, J., Choullarton, T. W., Westbrook, C. D., Blyth, aA. M., Bower, K. N., Connolly, P.
1013 J., Dearden, C., Gallagher, M. W., Cui, Z. and Nicol, J. C.: Microphysical properties of cold
1014 frontal rainbands, *Q. J. R. Meteorol. Soc.*, 140(681), 1257–1268, doi:10.1002/qj.2206, 2013.

- 1015 Curry, J. A., Pinto, J. O., Benner, T. and Tschudi, M.: Evolution of the cloudy boundary layer
1016 during the autumnal freezing of the Beaufort Sea, , 102(96), 1997.
- 1017 Curry, J. A., Rossow, W. B., Randall, D. and Schramm, J. L.: Overview of Arctic Cloud and
1018 Radiation Characteristics, *J. Clim.*, 9(8), 1731–1764, 1996.
- 1019 DeMott, P. J., Prenni, [aA](#), J., Liu, X., Kreidenweis, S. M., Petters, M. D., Twohy, C. H.,
1020 Richardson, M. S., Eidhammer, T. and Rogers, D. C.: Predicting global atmospheric ice
1021 nuclei distributions and their impacts on climate., *Proc. Natl. Acad. Sci. U. S. A.*, 107(25),
1022 11217–22, doi:10.1073/pnas.0910818107, 2010.
- 1023 Field, P. R., Heymsfield, A. J. and Bansemer, A.: Shattering and particle interarrival times
1024 measured by optical array probes in ice clouds, *J. Atmos. Ocean. Technol.*, 23(10), 1357–
1025 1371, doi:10.1175/JTECH1922.1, 2006.
- 1026 Grosvenor, D. P., Choulaton, T. W., Lachlan-Cope, T., Gallagher, M. W., Crosier, J., Bower,
1027 K. N., Ladkin, R. S. and Dorsey, J. R.: In-situ aircraft observations of ice concentrations
1028 within clouds over the Antarctic Peninsula and Larsen Ice Shelf, *Atmos. Chem. Phys.*,
1029 12(23), 11275–11294, doi:10.5194/acp-12-11275-2012, 2012.
- 1030 Herman, G. and Goody, R.: Formation and Persistence of Summertime Arctic Stratus Clouds,
1031 *J. Atmos. Sci.*, 33(8), 1537–1553, doi:10.1175/1520-
1032 0469(1976)033<1537:FAPOSA>2.0.CO;2, 1976.
- 1033 Hobbs, P. V. and Rangno, A. L.: Microstructures of low and middle-level clouds over the
1034 Beaufort Sea, *Q. J. R. Meteorol. Soc.*, 124(550), 2035–2071, doi:10.1002/qj.49712455012,
1035 1998.
- 1036 Intrieri, J. M.: An annual cycle of Arctic surface cloud forcing at SHEBA, *J. Geophys. Res.*,
1037 107, 8039, doi:10.1029/2000JC000439, 2002.
- 1038 [Jackson, R. C., McFarquhar, G. M., Korolev, A. V., Earle, M. E., Liu, P. S. K., Lawson, R.](#)
1039 [P., Brooks, S., Wolde, M., Laskin, A., and Freer, M.: The dependence of ice microphysics on](#)
1040 [aerosol concentration in arctic mixed-phase stratus clouds during ISDAC and M-PACE. *J.*](#)
1041 [Geophys. Res.](#), 117, D15207, doi:10.1029/2012JD017668, 2012
- 1042 Kahl, J. D.: Characteristics of the low-level temperature inversion along the Alaskan Arctic
1043 coast, *Int. J. Climatol.*, 10(5), 537–548, 1990.
- 1044 Korolev, A. V., Emery, E. F., Strapp, J. W., Cober, S. G., Isaac, G. A., Wasey, M. and
1045 Marcotte, D.: Small ice particles in tropospheric clouds: fact or artifact?, *Bull. Am. Meteorol.*
1046 *Soc.*, 92(8), 967–973, doi:10.1175/2010BAMS3141.1, 2011.
- 1047 [Korolev, A. V., Emery, E. and Creelman, K.: Modification and Tests of Particle Probe Tips](#)
1048 [to Mitigate Effects of Ice Shattering, *J. Atmos. Oceanic Technol.*, 30, 690–708, 2013](#)
- 1049 Lance, S., Brock, C. [aA](#), Rogers, D. and Gordon, J. [aA](#): Water droplet calibration of the
1050 Cloud Droplet Probe (CDP) and in-flight performance in liquid, ice and mixed-phase clouds

1051 during ARCPAC, *Atmos. Meas. Tech.*, 3(6), 1683–1706, doi:10.5194/amt-3-1683-2010,
1052 2010.

1053 [Lance, S., Shupe, M. D., Feingold, G., Brock, C. A., Cozic, J., Holloway, J. S., Moore, R. H.,](#)
1054 [Nenes, A., Schwarz, J. P., Spackman, J. R., Froyd, K. D., Murphy, D. M., Brioude, J.,](#)
1055 [Cooper, O. R., Stoh, A., and Burkhardt, J. F.:](#) *Cloud condensation nuclei as a modulator of ice*
1056 [processes in Arctic mixed-phase clouds](#) *Atmos. Chem. Phys.*, 11, 8003–8015, 2011
1057 www.atmos-chem-phys.net/11/8003/2011/ doi:10.5194/acp-11-8003-2011, 2011.

1058 Lawson, P. R.: The 2D-S (stereo) probe: design and preliminary tests of a new airborne high-
1059 speed, high resolution particle imager probe, *J. Atmos. Ocean. Technol.*, 23(1997), 1462–
1060 1477, 2006.

1061 [Lohmann, U. and Feichter, J.:](#) *Global indirect aerosol effects: a review*, *Atmos. Chem. Phys.*,
1062 [5](#), 715–737, 2005.

1063 McFarquhar, G. M., Um, J. and Jackson, R.: Small Cloud Particle Shapes in Mixed-Phase
1064 Clouds, *J. Appl. Meteorol. Climatol.*, 52(5), 1277–1293, doi:10.1175/JAMC-D-12-0114.1,
1065 2013.

1066 McInnes, K. and Curry, J.: Modelling the mean and turbulent structure of the summertime
1067 Arctic cloudy boundary layer, *Boundary-Layer Meteorol.*, 73(1), 125–143, 1995.

1068 Neiburger, M.: Reflection, absorption, and transmission of insolation by stratus cloud, *J.*
1069 *Meteorol.*, 6, 104, 1949.

1070 Overland, J. E. and Wang, M.: When will the summer Arctic be nearly sea ice free?,
1071 *Geophys. Res. Lett.*, 40(10), 2097–2101, doi:10.1002/grl.50316, 2013.

1072 Parkinson, C. L. and Comiso, J. C.: On the 2012 record low Arctic sea ice cover: Combined
1073 impact of preconditioning and an August storm, *Geophys. Res. Lett.*, 40(7), 1356–1361,
1074 doi:10.1002/grl.50349, 2013.

1075 [Rangno, A. L. and Hobbs, P. V.:](#) *Ice particles in stratiform clouds in the Arctic and possible*
1076 [mechanisms for the production of high ice concentrations](#), *J. Geophys. Res.*, 106(D14),
1077 [15065](#), doi:10.1029/2000JD900286, 2001.

1078 [Rogers, D. C., DeMott, P. J. and Kreidenweis, S. M.:](#) *Airborne measurements of tropospheric*
1079 [ice-nucleating aerosol particles in the Arctic spring](#), *J. Geophys. Res.*, 106(D14), 15053,
1080 doi:10.1029/2000JD900790, 2001.

1081 Rosenberg, P. D., Dean, [aA](#). R., Williams, P. I., Dorsey, J. R., Minikin, [aA](#)., Pickering, M.
1082 [aA](#)., & Petzold, [aA](#). (2012). Particle sizing calibration with refractive index correction for
1083 light scattering optical particle counters and impacts upon PCASP and CDP data collected
1084 during the Fenec campaign. *Atmospheric Measurement Techniques*, 5(5), 1147–1163.
1085 doi:10.5194/amt-5-1147-2012

Formatted: Font: Not Italic

Formatted: Font: Not Italic

1086 Tsay, S. and Jayaweera, K.: Physical characteristics of Arctic stratus clouds, J. Clim. Appl.
1087 Meteorol., 23(4), 584–596, 1984.

Formatted: Font: Not Bold

1088
1089
1090
1091
1092
1093
1094
1095
1096
1097
1098
1099
1100
1101
1102

Flight	Run Number	Time (UTC)	Altitude (m)	Temperature (°C)
B761	A1	13:13:26-13:16:43	1850 - 50	-19 to -5
B761	A2	13:04:40-13:10:33	300 - 1850	-8 to -19
B761	A3	13:23:20-13:33:19	1700-50	-19 to -7
B768	B1	11:45:16 - 11:54:02	1600 - 50	-17 to -9
B768	B2	11:38:39 - 11:44:59	50 - 1600	-17 to -4
B768	B3	12:01:30 - 12:19:08	400 - 50	-12 to -9
B768	B4	12:32:20 - 12:48:14	1300 - 1050	-16 to -14

M191	C1.1	08:53:45 - 09:00:00	~ 2950	~ -7
M191	C1.2	09:00:00 - 09:06:50	~ 2900	~ -6
M191	C1.3	09:06:50 - 09:13:35	~ 2750	~ -5
M191	C1.4	09:13:35 - 09:21:09	2750 - 2250	-4 to -2
M191	C2	10:14:58 - 10:33:51	3350 -2300	-7 to -3
M192	D1	12:58:58 - 13:06:02	3100 - 3750	-5 to -1
M192	D2	12:19:10 - 12:48:16	3100 - 3750	-5 to -1

Table 1: Flight numbers, run numbers, and their associated time intervals, altitude and temperature range for the four ACCACIA case studies presented.

1103

1104

1105

1106

Flight	Max Median Ice (L^{-1})	Min Median Temp (C)	Max RH (%)	CAS Aerosol Conc (cm^{-3})	PCASP Aerosol Conc (cm^{-3})	Predicted CAS IN value (L^{-1})	Predicted PCASP IN value (L^{-1})
Case 1a	0.61	-18.7	90.3	0.99 ± 0.25	3.13 ± 1.74	$1.02 \pm 1.14/0.88$	$1.80 \pm 2.25/1.20$
Case 1b	0.61	-18.7	22.16	0.14 ± 0.1	4.94 ± 2.22	$0.38 \pm 0.50/0.21$	$2.26 \pm 2.72/1.68$
Case 1c	0.61	-18.7	85.43	1.48 ± 0.37	4.04 ± 2.25	$1.24 \pm 1.34/1.08$	$2.05 \pm 2.55/1.37$
Case 2a	0.47	-16.2	69.68	1.50 ± 0.30	3.23 ± 1.68	$0.76 \pm 0.82/0.69$	$1.05 \pm 1.26/0.77$
Case 2b	0.47	-16.2	92.60	2.40 ± 0.32	4.96 ± 2.28	$0.93 \pm 0.98/0.87$	$1.27 \pm 1.49/0.97$
Case 2c	0.47	-16.2	93.86	2.07 ± 6.57	3.07 ± 1.86	$0.87 \pm 1.61/$	$1.03 \pm 1.26 /0.69$
Case 3a	3.35	-10	89.37	0.06 ± 0.07	-	$0.06 \pm 0.07/$	-
Case 3b	3.35	-10	59.66	0.15 ± 0.11	-	$0.08 \pm 0.09/0.05$	-
Case 3c	3.35	-10	89.79	0.33 ± 0.76	-	$0.10 \pm 0.13/$	-
Case 3d	3.35	-10	89.70	0.48 ± 0.21	-	$0.11 \pm 0.12/0.09$	-
Case 4a	2.50	-4.3	79.70	3.73 ± 1.03	-	$0.009 \pm 0.009/0.009$	-
Case 4b	2.50	-4.3	73.46	4.03 ± 0.58	-	$0.009 \pm 0.009/0.009$	-
Case 4c	2.50	-4.3	31.57	0.24 ± 0.14	-	$0.007 \pm 0.007/0.006$	-

1107 **Table 2.** Measurements of: aerosol concentrations $> 0.5 \mu m$ from the CAS and PCASP
1108 probes, together with predicted primary IN number using the DeMott et al. (2010) (*D10*)
1109 scheme (with either CAS or PCASP aerosol concentration data as input). Observed minimum
1110 median cloud temperatures were input to *D10*, and IN predictions were compared with
1111 observed maximum median ice concentrations.

1112

1113

1114

Flight	Mean Ice Conc (L ⁻¹)	Max ± std. dev. (60 sec) Ice Conc (L ⁻¹)	Temp of Max Conc (°C)	Max RH for Aerosol (%)	Observed Aerosol Conc (cm ⁻³)	Predicted IN Value (L ⁻¹)
Cloud Layers Over Larsen C						
99-i4	0.007 ± 0.002	0.017 ± 0.007/0.005	-13.8	50	0.33 ± 0.05	0.25±0.26/0.23
99-i5	0.007 ± 0.001	0.020 ± 0.007/0.004	-16.5	50	0.33 ± 0.05	0.41±0.44/0.39
104-i3	0.008 ± 0.002	0.012 ± 0.005/0.003	-17.7	40	0.15 ± 0.03	0.35±0.38/0.31
104-i4	0.011 ± 0.002	0.032 ± 0.010/0.007	-13.4	60	0.15 ± 0.03	0.17±0.18/0.16
Hallett Mossop Zone Ice						
100-i1	0.52 ± 0.02	1.28 ± 0.06/0.38	-0.7	75	0.42 ± 0.05	1.9×10 ⁻⁵
100-i2	1.14 ± 0.02	3.44 ± 0.11/1.01	-2.3	75	0.42 ± 0.05	9.1×10 ⁻⁴
100-i3	1.47 ± 0.02	6.26 ± 0.15/1.78	-4.3	75	0.42 ± 0.05	0.007
100-i4	0.90 ± 0.02	4.77 ± 0.12/1.28	-5.9	75	0.42 ± 0.05	0.019
100-i5	0.05 ± 0.01	0.06 ± 0.01/0.01	-5.6	75	0.42 ± 0.05	0.016
100-i6	0.040 ± 0.008	0.07 ± 0.01/0.03	-5.2	75	0.42 ± 0.05	0.013
104-i5	0.098 ± 0.007	0.37 ± 0.03/0.12	-2.3	94	0.1 ± 0.05	8.3x10 ⁻⁴
104-i6	0.33 ± 0.01	2.7 ± 0.01/0.63	-2.3	94	0.1 ± 0.05	8.3x10 ⁻⁵

Formatted: Font: 8 pt

Formatted: Font: 8 pt

Formatted: Font: 8 pt

Formatted: Font: 8 pt

Formatted: Font: 8 pt

Formatted: Font: 8 pt

Formatted: Font: 8 pt

Formatted: Font: 8 pt

Formatted: Font: 8 pt

Formatted: Font: 8 pt

Formatted: Font: 8 pt

Formatted: Font: 8 pt

Formatted: Font: 8 pt

Formatted: Font: 8 pt

Formatted: Font: 8 pt

Formatted: Font: 8 pt

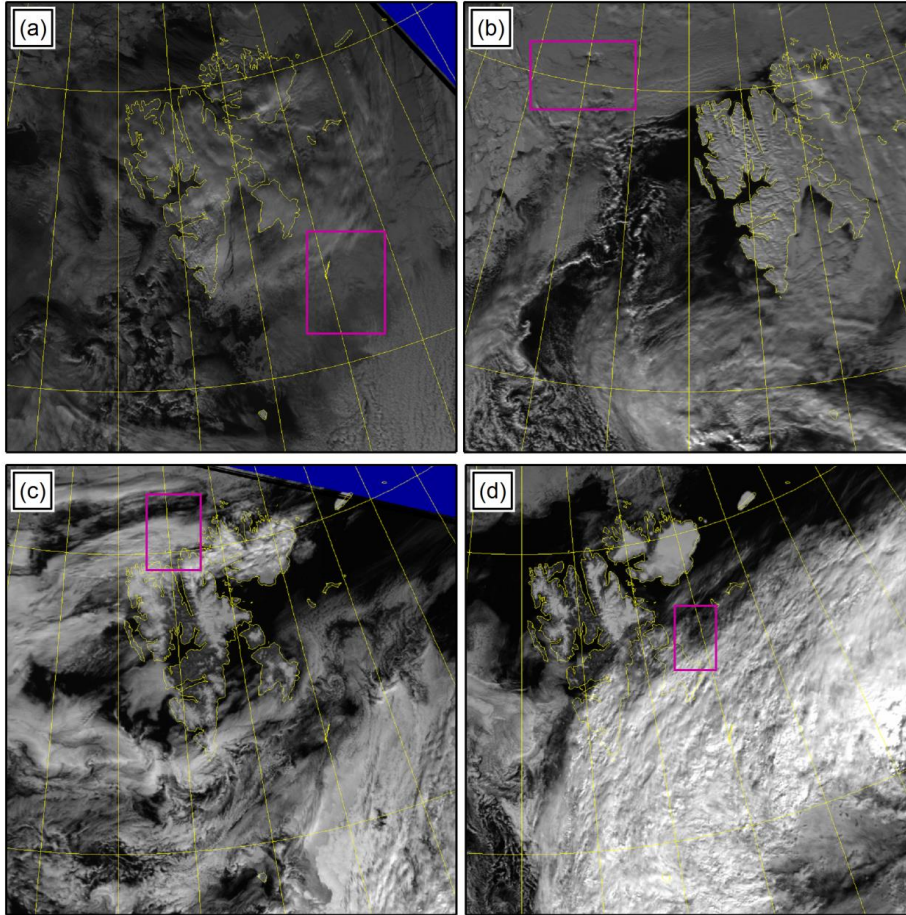
Formatted: Font: 8 pt

Formatted: Font: 8 pt

Formatted: Font: 8 pt

Formatted: Font: 8 pt

1115 **Table 3:** Table reproduced from Grosvenor et al. (2012) reporting observations of ice number
1116 concentrations, aerosol concentrations > 0.5µm and primary IN predictions using the *D10*
1117 parameterisation.



1118

1119 **Fig 1:** AVHRR visible satellite imagery for spring case 1 (a), spring case 2 (b), summer case
1120 1 (c) and summer case 2 (d). Science flight area highlighted by purple boxes in each figure.

1121

1122

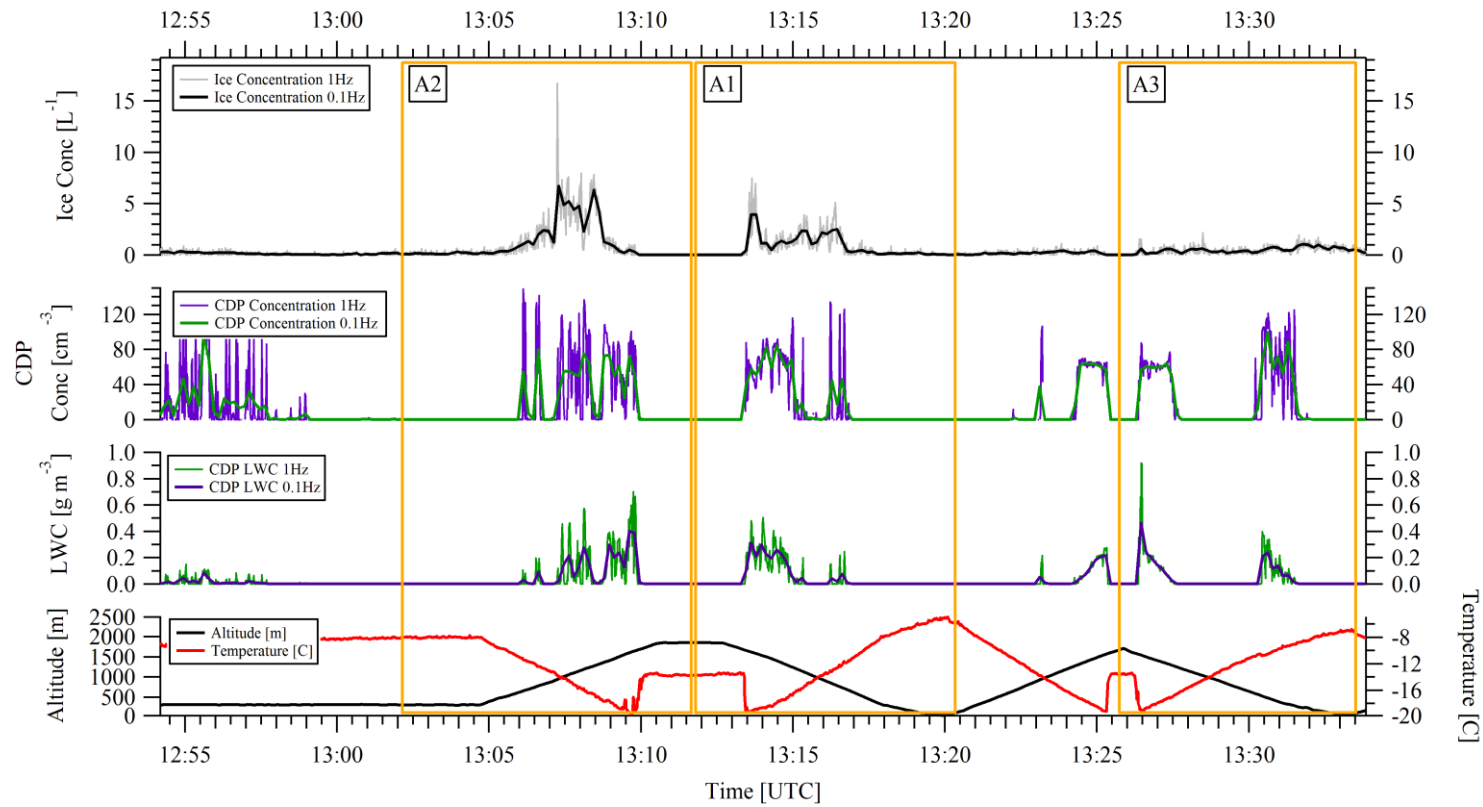


Fig 2: Microphysics time series for spring case 1. Data includes temperature (°C) and altitude (m) (lower panel) together with 1 and 10 second data sets for CDP liquid water content (g m^{-3}) (panel 2 from bottom), CDP cloud particle number concentration (cm^{-3}) (panel 3), and ice water content (g m^{-3}) and ice number concentrations (L^{-1}) (top panel). Profiles A2 and A3 are described in Appendix A

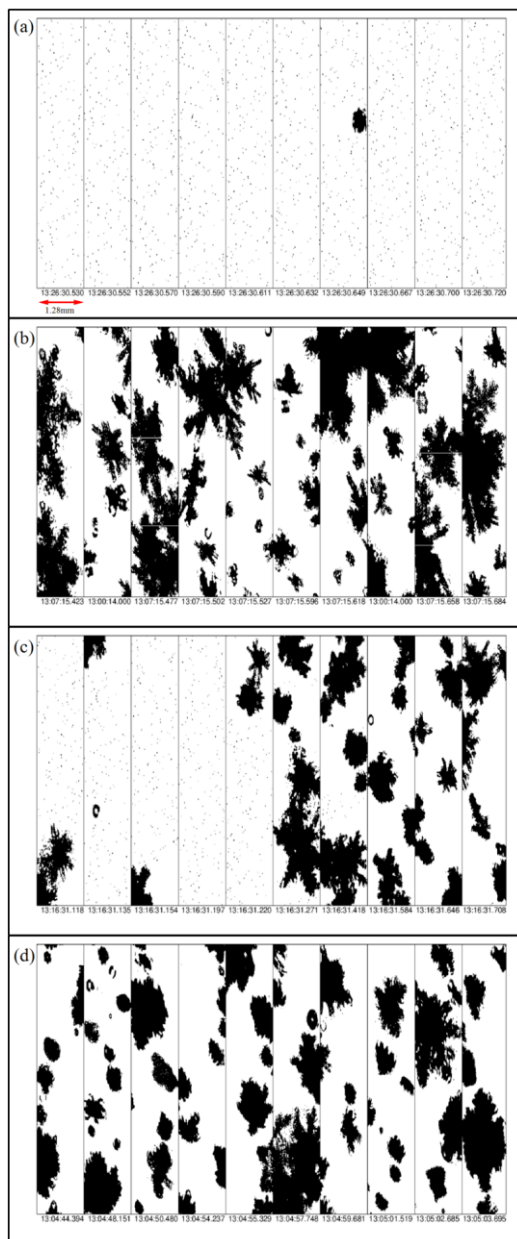


Fig 3. Images from the 2D-S cloud probe during spring case 1 from: (a) a cloud top region during A1 ; (b) 500 m below cloud top during A2 ; (c) region of swift transitions between ice and liquid and (d) precipitation region below cloud base .

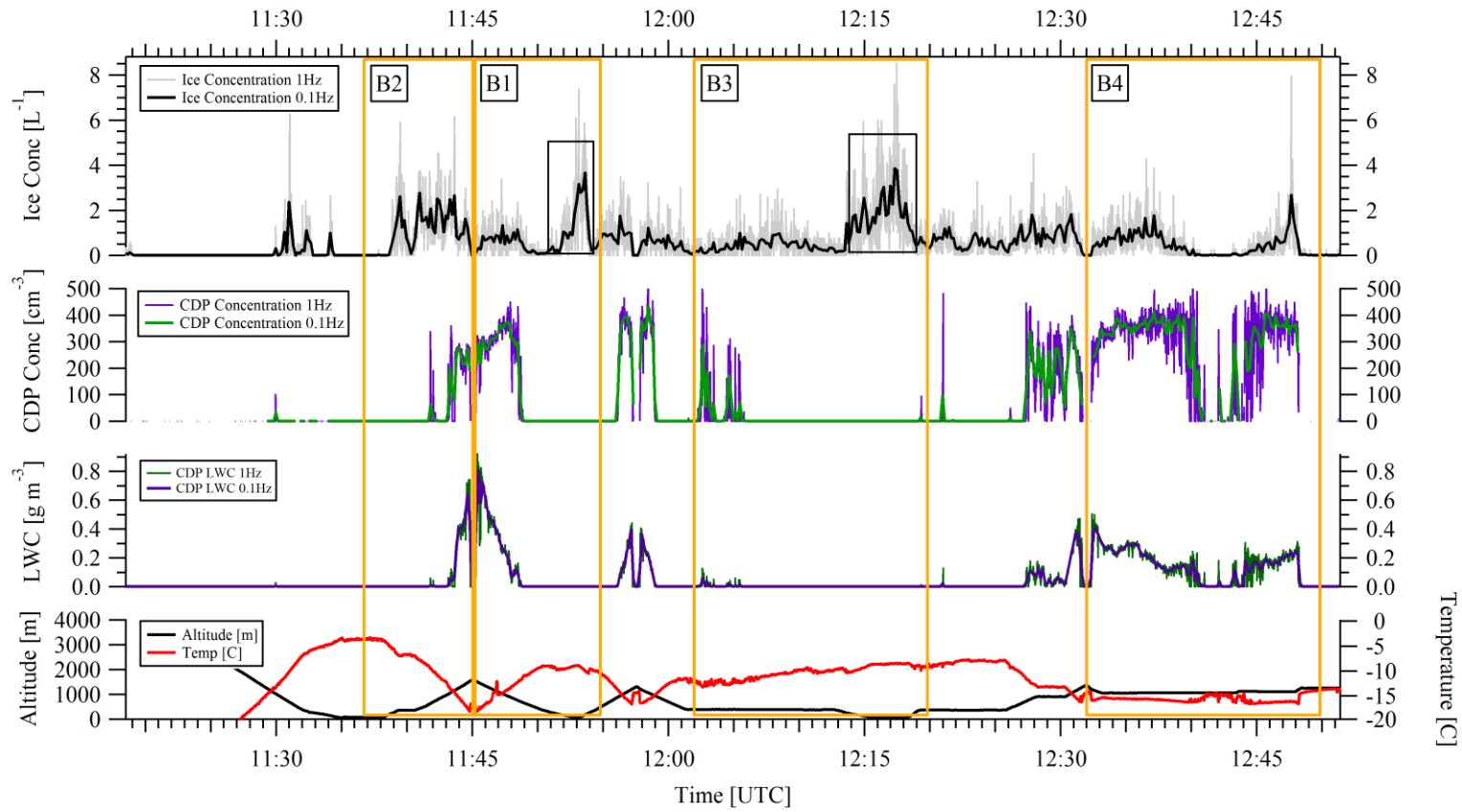


Fig. 4: Microphysics time series data for spring case 2. Data includes temperature (°C) and altitude (m) (lower panel) 1 and 10 second data sets for CDP liquid water content (g m^{-3}) and CDP concentration (cm^{-3}) (middle panels), and ice water content (g m^{-3}) and ice number concentrations (L^{-1}) (top panel). Profiles B2, B3 and B4 are described in Appendix B

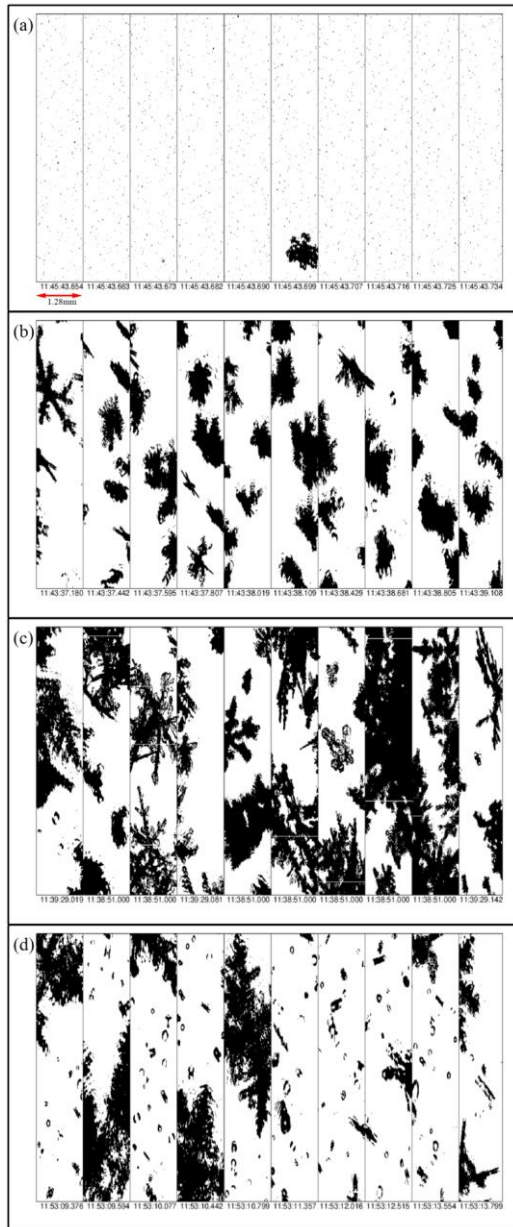


Fig. 5: Images from the 2D-S cloud probe from spring case 2 for: (a) cloud top during B1 ; (b) profiled ascent during B2; (c) dendritic ice in the cloud base region during B2 and (d) columnar ice above the sea surface during B2

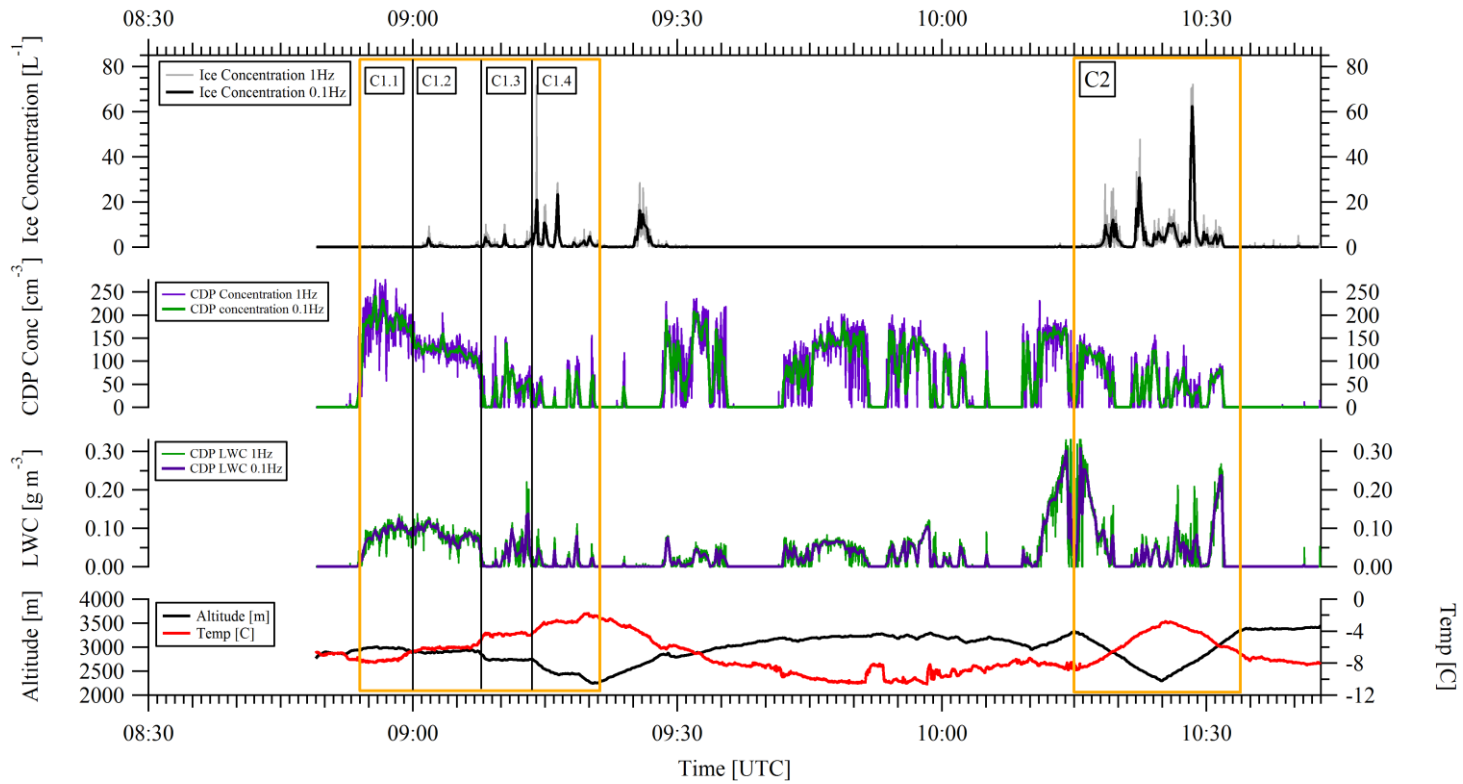


Fig. 6 Microphysics time series data for summer case 1. Data includes temperature (°C), altitude (m) (lower panel) together with 1 and 10 second data sets for CDP liquid water content (g m^{-3}) (second panel up), CDP concentration (cm^{-3}), ice water content (g m^{-3}) and ice number concentrations (L^{-1}) (top panel). Flight segments C1.1, C1.2, C1.3 and C1.4 are described in Appendix C.

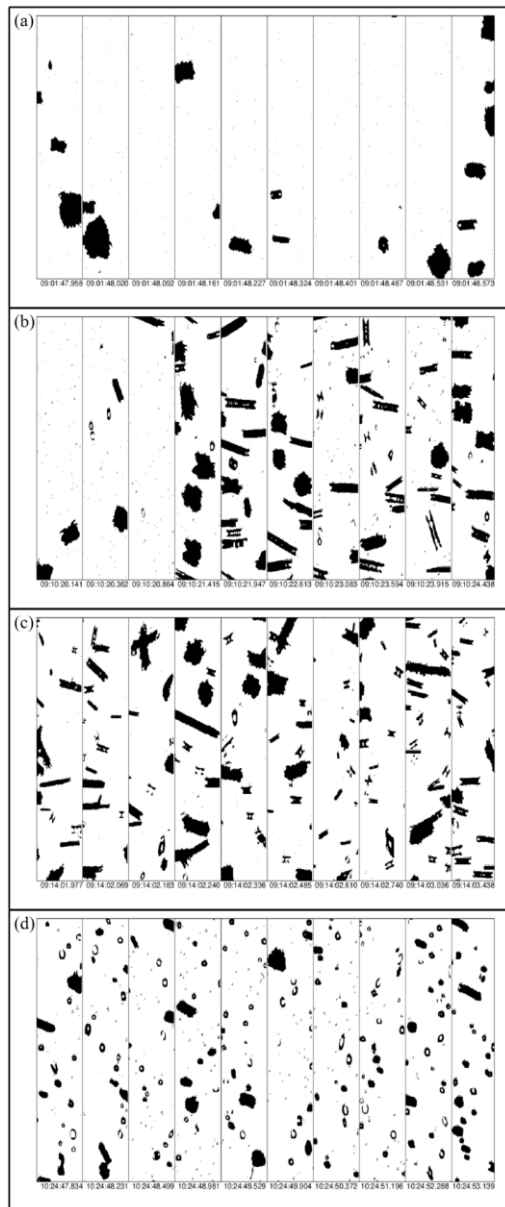


Fig. 7. Images from the 2D-S cloud probe from summer case 1 for: (a) small irregular ice during C1.2 ; (b) and (c) secondary ice production during C1.3 and C1.4 respectively, and (d) ice together with drizzle during C2.

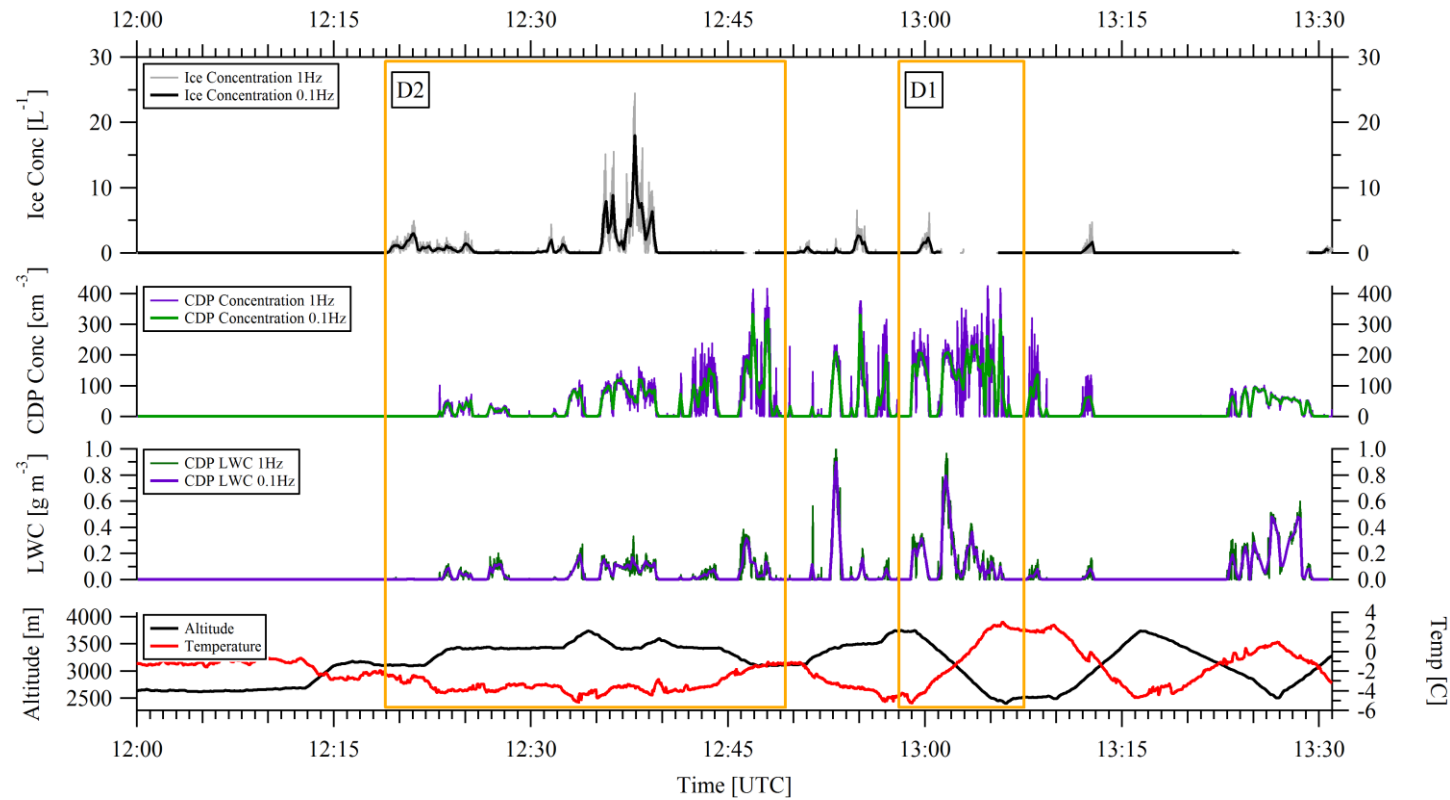


Fig. 8: Microphysics time series data for summer case 2. Data includes temperature ($^{\circ}\text{C}$), altitude (m) (lower panel) together with 1 and 10 second data sets for CDP liquid water content (g m^{-3}), CDP concentration (cm^{-3}) (middle panels), ice water content (g m^{-3}) and ice number concentrations (L^{-1}) (top panels). Profile D1 is described in Appendix D

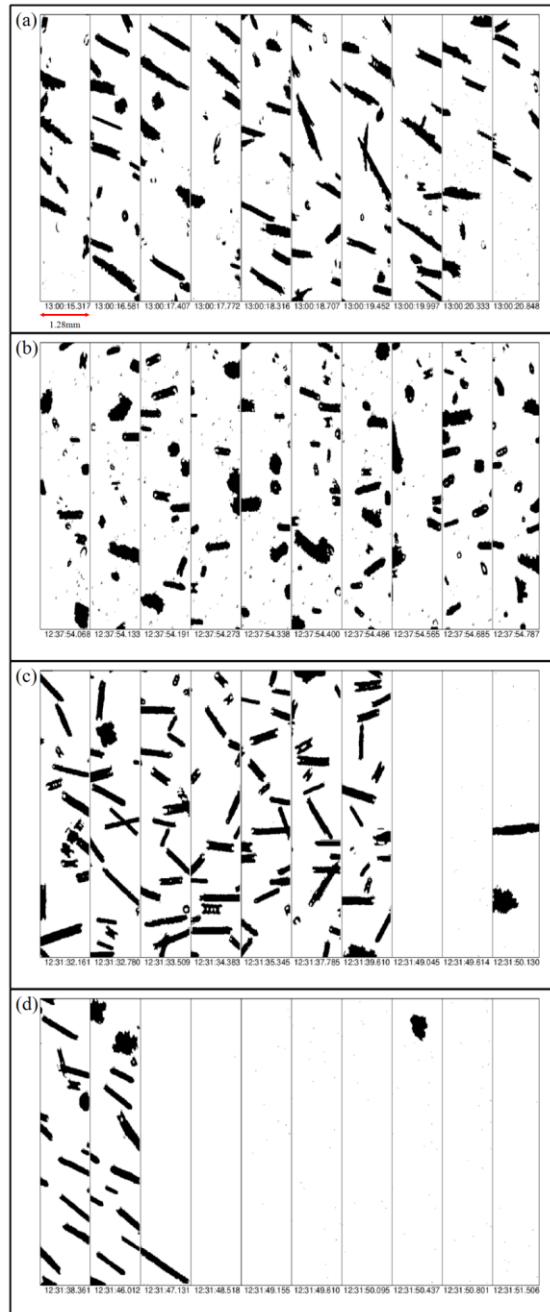


Fig. 9: 2D-S cloud probe imagery for summer case 2 showing: (a) columnar ice during D1 ; (b) images of columns together with liquid during D2 and swift transitions between (c) glaciated and (d) liquid phases during D2.

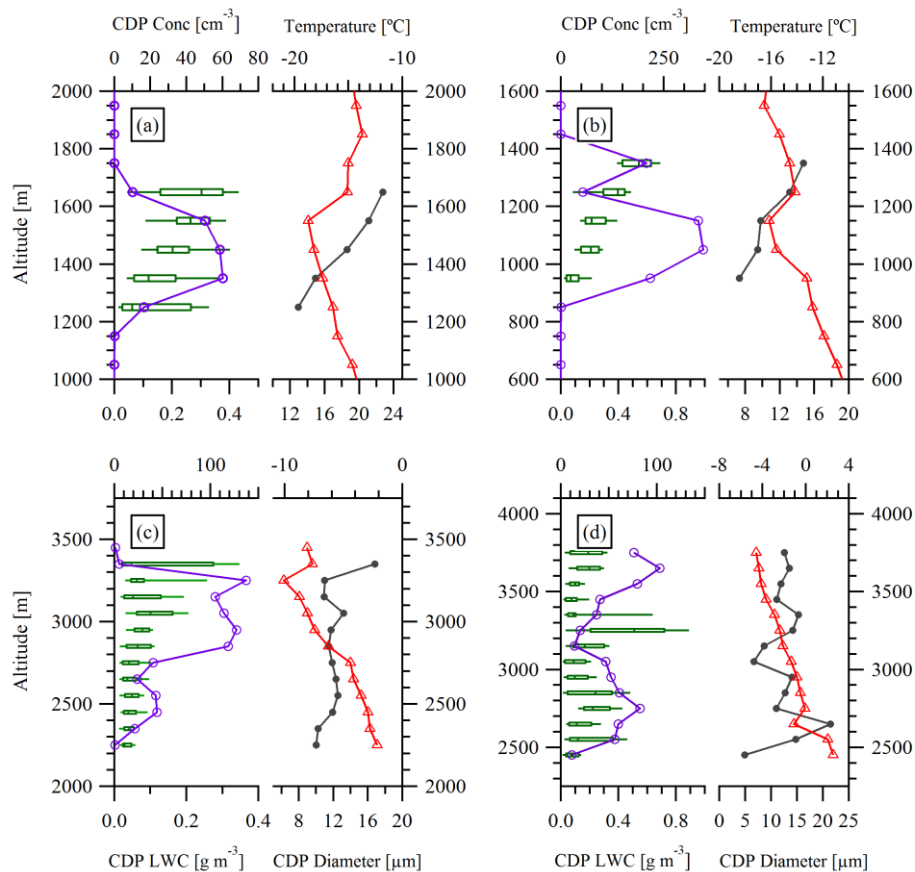


Fig. 10: Percentile plots (50th, 25th, 75th percentiles, whiskers to 10 and 90%) as a function of altitude for LWC from CDP (green), and median droplet number concentration (purple), median droplet diameter (grey) and median temperature (red). Data are averaged over 100 m deep layers. Figs. (a - d) are for Spring Case 1, Spring Case 2, Summer Case 1 and Summer Case 2 respectively.

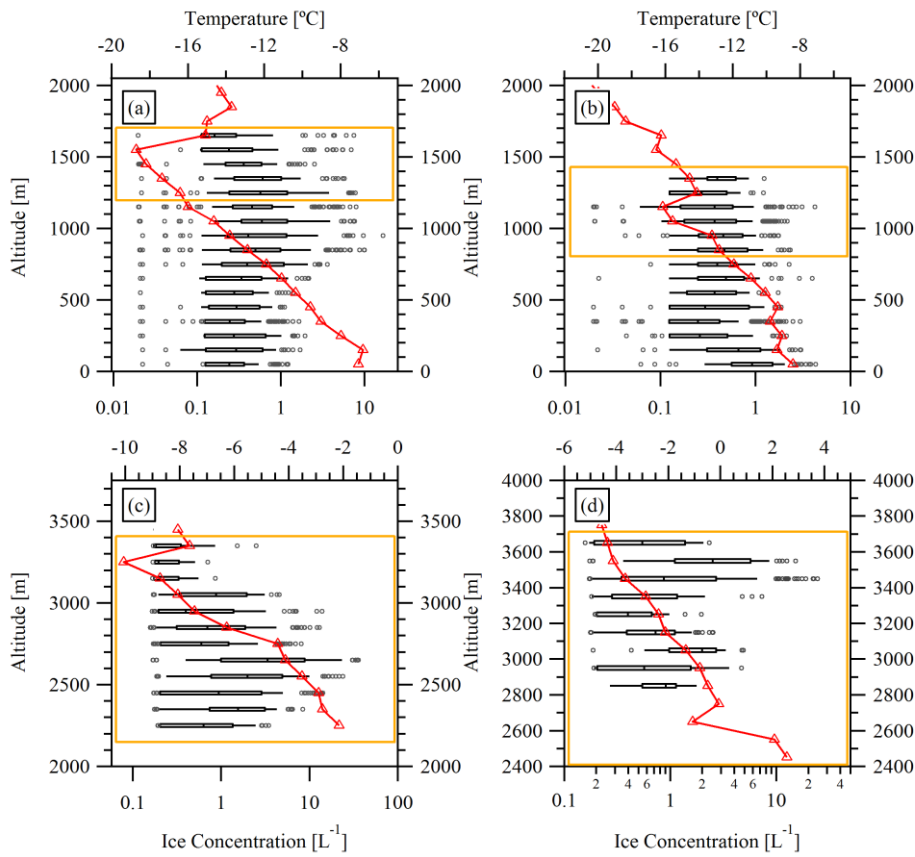


Fig. 11: Box and whisker plots with 50th, 25th, 75th percentiles, whiskers to 10 and 90% and outliers between 95 and 100% as a function of altitude for ice number concentrations (black) and median temperature (red) (Figs. (a-d) and altitude averages as in Fig. 10 above). The box in yellow provides an indication of the full extent of cloud layers investigated. Figs. (a - d) are for Spring Case 1, Spring Case 2, Summer Case 1 and Summer Case 2 respectively.

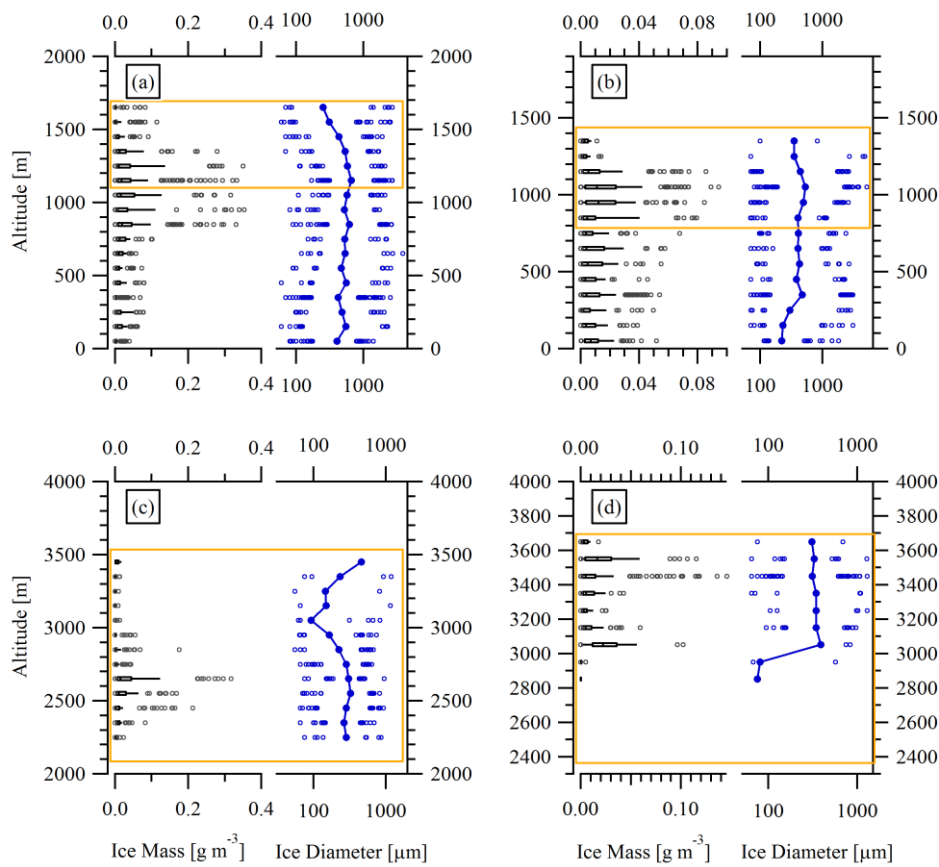


Fig. 12: Box and whisker plots with 50th, 25th, 75th percentiles, whiskers to 10 and 90% and outliers between 95 and 100% as a function of altitude for ice mass (black) and median ice crystal diameter with outliers between 95 and 100% (blue). (Figs. (a-d) and altitude averages as in Fig. 10 above). The box in yellow provides an indication of the full extent of cloud layers investigated. Figs. (a - d) are for Spring Case 1, Spring Case 2, Summer Case 1 and Summer Case 2 respectively.